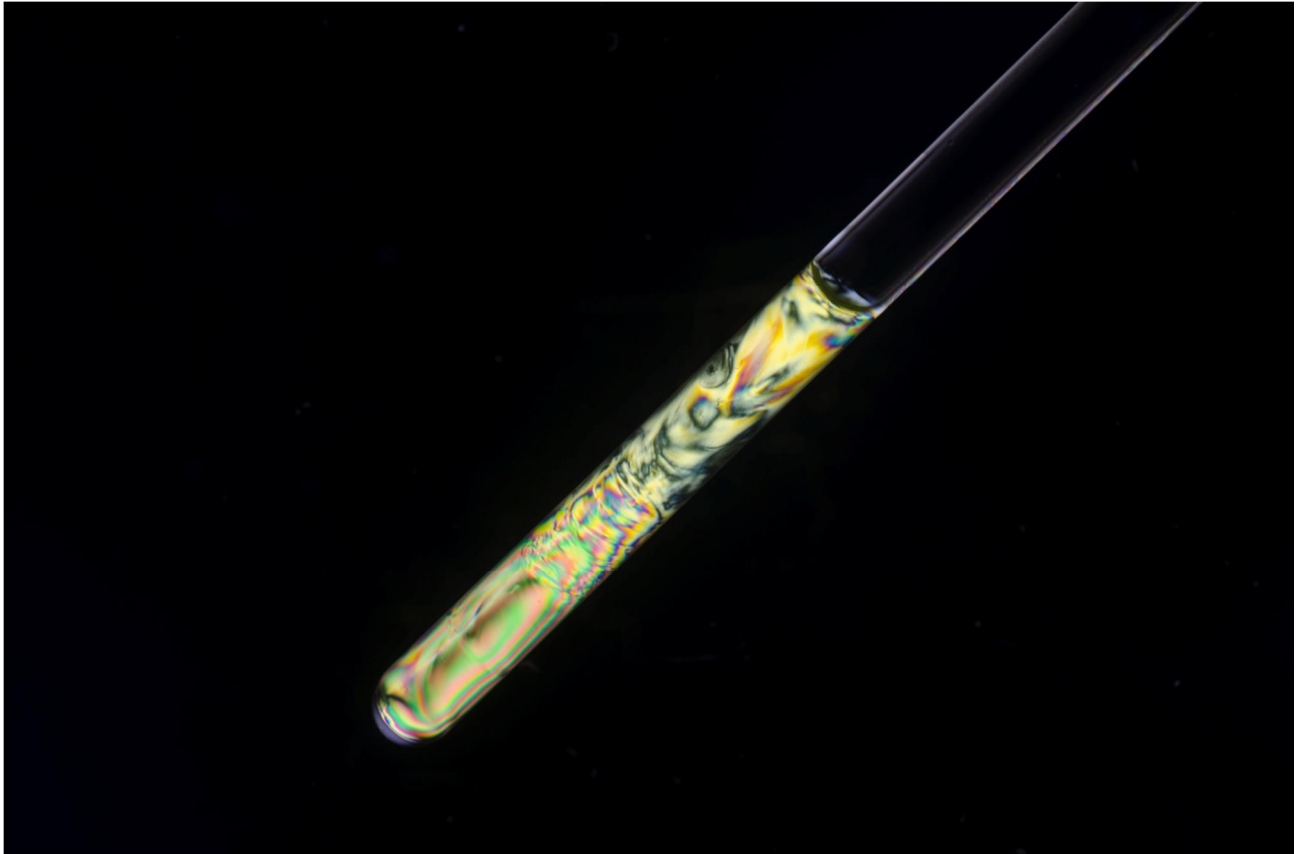




CHALMERS
UNIVERSITY OF TECHNOLOGY



Magnetic orientation of clays in aqueous glycerol and polymer solutions

Master's thesis in Materials Engineering Programme

Shiyu Geng

MASTER'S THESIS

Magnetic orientation of clays in aqueous glycerol and polymer solutions

60 hp Master's thesis within the Materials Engineering Programme
Course code: KBTX60

by Shiyu Geng

Department of Chemical and Biological Engineering
Division of Applied Chemistry, Chalmers University of Technology
Gothenburg, Sweden, August, 2014

Supervisor: Christoffer Abrahamsson (PhD student), Applied Chemistry,
Department of Chemical and Biological Engineering, Chalmers University of
Technology, Gothenburg, Sweden

Examiner: Michael Persson (Adjunct Professor), Applied Chemistry,
Department of Chemical and Biological Engineering, Chalmers University of
Technology, Gothenburg, Sweden and Innovation Manager, Akzo Nobel PPC,
Bohus, Sweden

Cover image:

Image of an NMR tube with an aqueous nontronite clay dispersion with a clay concentration of 2.1 wt% that was imaged between crossed polarizers with a Nikon D3200 camera, Nikon Corp with a Nikon AF-S 40 mm f/2.8 G objective.

Department of Chemical and Biological Engineering

Chalmers University of Technology

SE-412 96, Gothenburg, Sweden

Telephone +46 (0)31-772 1000

Abstract

Clays and liquid dispersions of individual clay plates are used in the synthesis of nanocomposite materials, where they are used to improve optical, mechanical and barrier properties. These properties can be further improved if the clay plates are collectively oriented in one direction. This thesis focuses on how the magnetic orientation of the clay plates in aqueous colloidal nontronite dispersions is affected by the clay concentration and the addition of solvent viscosity modifying agents, such as glycerol and polymethacrylamide. The dispersions phase behaviour, magnetic alignment, micro- and macro rheological properties were analysed by observation between crossed polarizers, inverted tube test, rheological measurements and relaxation measurements. An increased clay concentration resulted in a higher birefringence intensity and longer relaxation time. Small additions of glycerol produced shorter relaxation times. However increasing additions of glycerol increased the viscosity and relaxation time of the sample. The moduli and viscosity of the clay-glycerol system decreased from low to moderate clay concentrations and reached a minimum. This is attributed to the nematic-like phase formation in the moderate clay concentration range. It is also possible that the increased presence of counter ions associated with the clay plates caused screening of the electric double layers at moderate clay concentration, resulting on a more mobile system. Interestingly, the relaxation time predicted well with samples that can be aligned or not in a magnetic field. However, a comparison between relaxation times and macro-rheological properties such as viscosity did not correlate well. The addition of increasing amounts of polymethacrylamide to the dispersions with low and moderate clay concentration induced lower birefringence intensity and shorter relaxation time. In case of dispersions with high clay concentration, the alignment and relaxation behaviours of clay particles caused by increasing polymer concentration were far from trivial, possibly due to clay excluded volume effects.

Table of contents

Table of contents	7
1 Introduction	1
1.1 Clays and the next generation of nanocomposite materials.....	1
1.2 Scope of project.....	1
2 Background	3
2.1 Colloidal systems	3
2.2 Birefringence.....	10
3 Materials and Methods.....	11
3.1 Materials	11
3.2 Sample formulation and phase diagrams	11
3.3 Observations of samples between crossed polarizers.....	13
3.4 Rheological observations with inverted tube test.....	13
3.5 Protocol of rheological measurement with rheometer.....	13
3.6 Investigating relaxation of clay particles	15
4 Results.....	16
4.1 Colloidal system consisting of NAm s2 clay and aqueous glycerol solution	16
4.2 Colloidal system consisted of NAm s2 clay and aqueous PMAAm dispersion	30
5 Discussion	35
5.1 Clay concentration, magnetic alignment and birefringence relaxation time	35
5.2 Clay concentration, macro-rheology and its correlation to relaxation time	35
5.3 Glycerol concentration, magnetic alignment and birefringence relaxation time	36
5.4 Glycerol concentration, macro-rheology and its correlation to relaxation time	37
5.5 Sedimentation and phase separation.....	38
5.6 Influence of salt for magnetic alignment and relaxation time	38
5.7 Variation of pH in clay-glycerol dispersions	38
5.8 PMAAm concentration, magnetic alignment and birefringence relaxation time	39
6 Conclusion	40
Acknowledgements	41
References.....	42

1 Introduction

1.1 Clays and the next generation of nanocomposite materials

Colloidal clay dispersions and clay nanocomposites hydrogels holds a promise of replacing fossil fuel derived polymer solutions and gels in a number of applications. In the industry clay dispersions, by themselves or with additives, are used for a range of purposes such as oil well drilling, food packaging and sealing barriers for waste dumps or nuclear waste containment.¹ Clays can form stable nanoparticle dispersions or nanoparticle hydrogels in a liquid medium such as water or an organic solvent depending on surface chemistry of the clay particles. A commonly used family of clays are the smectite clays. These clay particles are impermeable to most diffusing substances and their large aspect ratio make them efficient diffusion barriers when dispersed as the second phase in composite materials.² In addition they are efficient in mechanically reinforcing materials making them popular for use in novel composites³. Relatively small amounts of clay added to liquids can cause large changes to the liquids rheology, due to this clay dispersions are used as water-based drilling fluids in oil and gas production processes.⁴

Nanocomposite materials based on clays has previously be used for controlled release of drugs⁵, pesticides⁶ and herbicides⁷ with the purpose of providing an extended and controlled level of substance release. The release from these clay composites can be adjusted by modifying surface chemistry of the clays and thereby the interaction between the diffusing substance and the clay surfaces. Furthermore, the release also depends of clay volume fraction and on geometrical factors such as clay plate shape, size distribution, aspect ratio and orientation. The impermeable clay plates form a tortuous pathway for a diffusing substance which length can be adjusted by changing the orientation of the clays. Three basic states of clay plate orientation can be defined relative the direction of diffusive flux: parallel, random and perpendicular orientation, where the first obstruct the diffusion the least and the last the most. The orientation of clays can be changed in a number of ways, for example by exposing the sample to electric or magnetic fields.²

1.2 Scope of project

1.2.1 *Purpose*

In this thesis two types of colloidal dispersions are investigated, the first consist of nontronite clay plates and glycerol while the second consists of nontronite clay plates and polymer which has upper critical solution temperature (UCST). The purpose of this study is to better understand how the rheological properties of the colloidal particle/polymer/solvent dispersion influence the magnetic alignment of the plate-shaped nontronite particles. Another purpose is to find a way to reversibly induce anisotropy in the microstructure of the gels. This would create an ON-OFF switch that affects several characteristics that depends on microstructure orientation in a sample, such as optical, mechanical and liquid mass transport properties.

1.2.2 *Goal*

The first goal is to investigate how the rheological properties of clay-water-glycerol dispersions influence the magnetic alignment of the clay particles. The second goal is to formulate a temperature responsive sol-gel system that can be used to achieve reversible magnetic orientation of nontronite clay.

The temperature responsiveness will be accomplished by varying the temperature in dispersions containing exfoliated clay particles and water-soluble and temperature responsive polymers. The mixture is a gel at room temperature that locks the clays into their positions. However, when heating the material the gel goes into a dispersion making it possible to change the orientation clays by magnetic fields. After clays have been reoriented the dispersion is allowed to cool and gel, again locking the clays into place, but now in a new orientation. This reversibly magnetic orientation of clays can be used to, for example, vary the mass transport of solvents and diffusants through the material.

2 Background

2.1 Colloidal systems

A colloidal system has at least one component that has at least one dimension within nanoscale (10^{-9} m) to microscale (10^{-6} m). Broadly, microscopic particles forming one phase dispersed in a liquid phase are called colloidal sols or dispersions. The properties of colloidal sols are often related to the high surface area of dispersed phase and chemical nature of particle's surface.⁸ For the charged colloids in dispersion the surface charge influences the distribution of nearby ions in the polar medium by attracting and repelling oppositely and similarly charged ions, respectively.⁹ Polymer solutes steric forces may play a role in modulating interparticle forces, producing an additional steric repulsive force or an attractive depletion force between them.^{10, 11}

2.1.1 *Nontronite and its dispersions*

2.1.1.1 *Definition and structure of nontronite particles*

Nontronite is a naturally occurring swelling di-octahedral clay mineral, which is a member of the montmorillonite-beidellite series. The clay consist of one octahedral layer containing ions such as Mg^{2+} or Al^{3+} and Fe^{3+} sandwiched between two tetrahedrally structured silica layers that also host cations. Figure 1 illustrates the crystal structure of nontronite. The structural formula of nontronite is $(\text{Si}_{7.55}\text{Al}_{0.16}\text{Fe}_{0.29})(\text{Al}_{0.34}\text{Fe}_{3.54}\text{Mg}_{0.05})\text{O}_{20}(\text{OH})_4\text{Na}_{0.72}$ and the density of the nontronite as estimated from the unit-cell parameters is about 3.0 g/cm^3 .¹² When the octahedral or tetrahedral cations are replaced by lower valent cations, the clay faces become negatively charged. For example, in nontronite most of aluminium atoms are replaced by iron ions. Interlayer cations are present close to the clay surfaces of the clay sheets to balance the negative charge. On the clay edges, there are octahedral Al-OH and tetrahedral Si-OH groups. As shown in Figure 2, the charges of these amphoteric sites are variable at different pH environments, due to H^+ or OH^- transfer from the aqueous phase.¹³

2.1.1.2 *Properties of nontronite dispersions*

Aqueous colloidal nontronite dispersions have previously been investigated by Laurent J. Michot and co-workers^{12, 14, 15} where they studied the gel structure and mechanical properties of these dispersions. They observed isotropic/nematic/gel transitions when varying clay and salt concentration.

An isotropic clay dispersion has particles that are evenly distributed and randomly oriented. This is different from the nematic phase that is the simplest liquid-crystalline phase. In a nematic phase the anisotropic clay particles are locally oriented in the same direction, while their centres of mass are not located on a lattice. This means nematic phase has long-range orientational order and only short-range positional order.¹⁶ The I/N transition of nontronite is influenced by many

factors, such as degree of particle anisotropy, concentration of nontronite, salt concentration, pH, temperature and aging.^{14, 17}

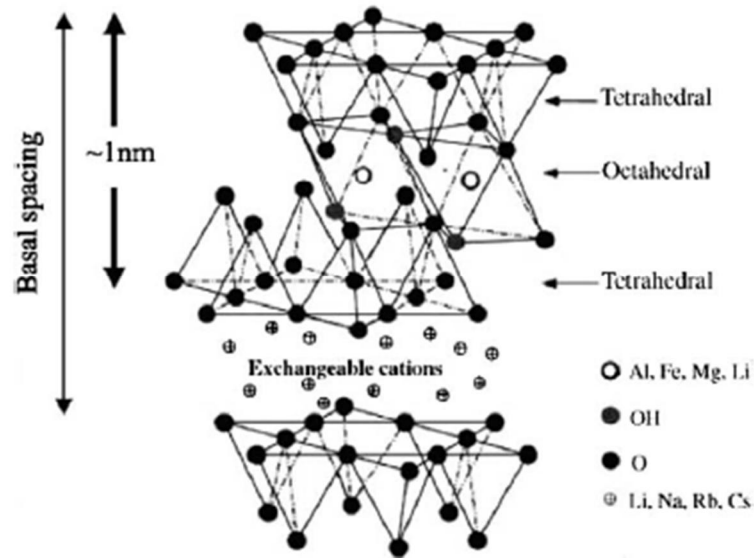


Figure 1 The nontronite crystal structure¹⁸ (Reprinted from Ref. 18, with permission from Elsevier, copyright 2003)

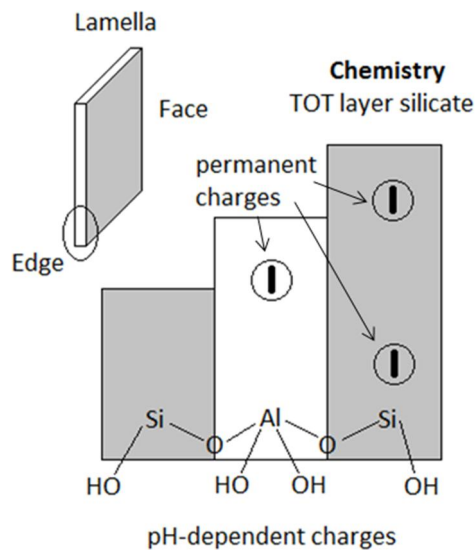


Figure 2 Schematic of clay structure and chemistry (Reprinted from Ref. 13, with permission from Elsevier, copyright 2004)

Commonly, clay dispersions experience the rheological property called thixotropy. One sign of thixotropy is that when the sample is sheared, its viscosity decreases continuously with time. Oppositely, when the flow is discontinued, the viscosity of the sample recovers with time. This

rheological behaviour is often theorized to be caused by microstructure changes that depend on the history of the sample.¹⁹

Nontronite clay particles aggregate in different ways depending on the salt concentration in the dispersion. Compared to dispersions with no salt, a low salt concentration often result in a decrease of the yield stress and viscosity to a minimum. This is because the electric double layer around the particles is slightly screened by salt ions which shrinks the effective volume of the clay particles, making it easier for the clay sheets to move.²⁰ At moderate salt concentration edge-to-face flocculation occurs because of electrostatic attraction between negative faces and positive edges of adjacent clay sheets. This kind of flocculation is rapid and results in loose flocculates, which exhibits no flow birefringence. At high salt concentration on the other hand, clay particles arrange face-to-face in a lamellar fashion and the dispersions exhibit streaming birefringence.²⁰ Such flocculation is slower but it gives more dense sediments.²¹

Due to the presence of ferric iron in the octahedral layer, nontronite dispersions are very sensitive to magnetic fields. The magnetic alignment is even easier if the phase is nematic as this enables collective movement of all the clays sheets in the whole phase.¹² The alignment of the dispersions can be observed between crossed polarizers as this gives the samples optical birefringence.²

2.1.2 *Glycerol and its aqueous solutions*

Glycerol is a viscous, colourless, sweet tasting liquid that is a by-product from soap manufacturing. The molecular formula of glycerol is HO-CH₂CHOH-CH₂OH and the molecular structure is illustrated in Figure 3. Recently, propylene and sucrose have been used for synthesizing glycerol. Glycerol is also used in the industry to produce alkyd resins and urethane polymer.²²

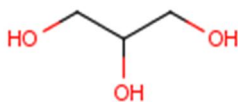


Figure 3 The chemical structure of the glycerol molecule

Glycerol has a density of 1.26 g/cm³ and is miscible with water. The viscosity of aqueous glycerol solutions is affected by the concentration of glycerol and temperature. Figure 4 and Figure 5 show the viscosity of glycerol/water mixtures at different glycerol concentrations and temperatures.²³

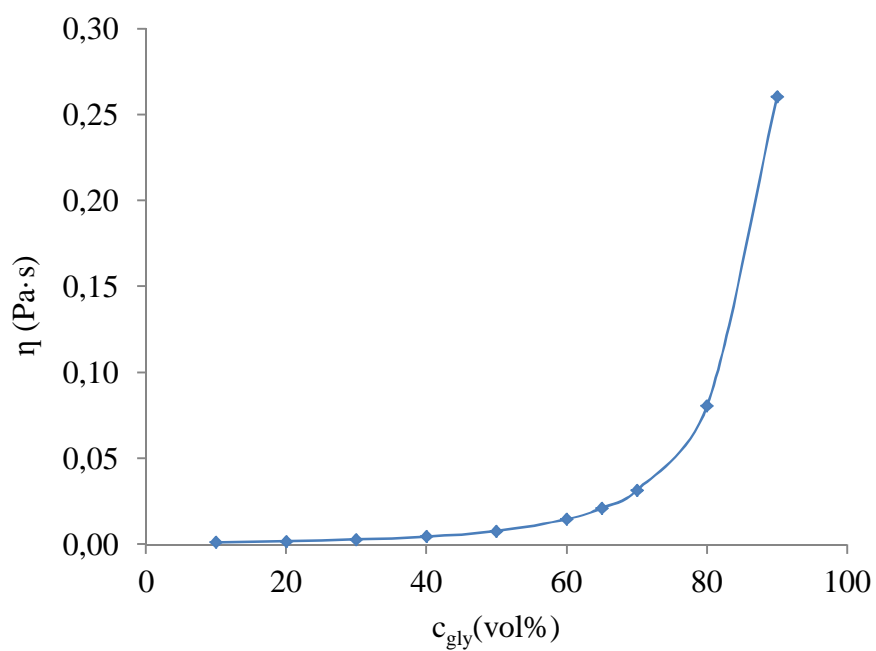


Figure 4 Viscosity of aqueous glycerol solutions with increasing glycerol concentration at 22°C. Data in figure is calculated at an online source²⁴.

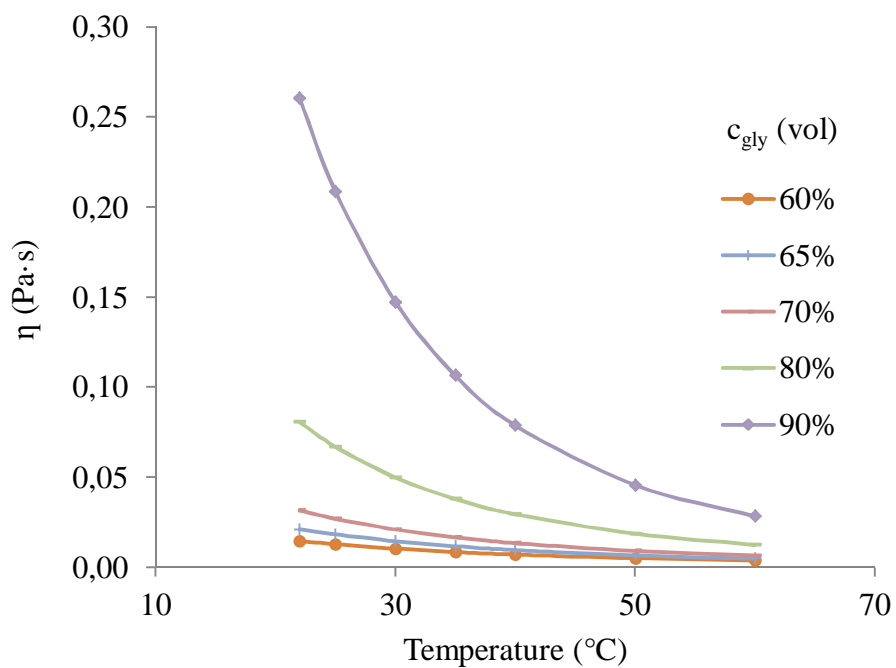


Figure 5 Viscosity of aqueous glycerol solutions at different temperatures. Data in figure is calculated at an online source²⁴.

As already described, one of the goals of this project was to combine UCST polymers and nontronite clays to produce a colloidal system in which the clay plates can be reversibly realigned in response to heating in a magnetic field. The combination of a thixotropic clay and a temperature responsive polymer forms a fairly complex system. Therefore the project started to investigate a system that was judged to be slightly less complex but still scientifically interesting. This system was the nontronite clay-glycerol system. Similarly to the polymer system, glycerol can change the viscosity of the dispersion but as glycerol is a smaller and simpler molecule it was hypothesized to be less likely to cause bridge flocculation of clay plates. As such it provided a good system to familiarize with before introducing the UCST polymer.

2.1.3 *Polymethacrylamide*

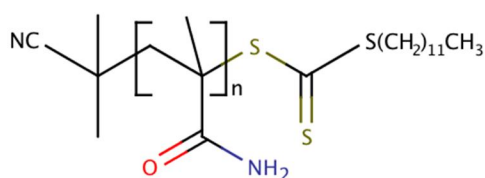


Figure 6 The chemical structure of PMAAm used in this research

Polymethacrylamide (PMAAm, Figure 6) is a thermoresponsive polymer having an UCST, which is the temperature at which the solution goes from an opaque to transparent state. The UCST is caused by the thermally reversible hydrogen bondings in the polymer. Silberberg et al.²⁵ proved the presence of intra- and intermolecular hydrogen bonds in dilute aqueous PMAAm solutions at low temperature by temperature-dependent light scattering experiments. These hydrogen bonds cause aggregation of the polymer molecules and the PMAAm solution is cloudy at a temperature below UCST. On the other hand, heating breaks the hydrogen bonds so the solution becomes a clear one phase solution at a temperature over UCST.²⁶ Because of the UCST character, the viscosity of PMAAm solutions is expected to be higher at low temperature compared to high temperature. The UCST of the PMAAm solution should not be seriously influenced by salt concentration since it is mainly caused by hydrogen bonding.

2.1.4 *Interactions between nontronite and various solvents*

Below the different forces of interest between the components in the samples are discussed.

2.1.4.1 *Ion dipole interactions*

The charged clay surfaces can adsorb the polar non-ionic molecules by ion-dipole interactions. Both water and glycerol molecules are dipoles and interact with charged clay surfaces. This kind of interaction depends on the hydration state of the clay and the nature of the exchangeable cation.²⁷

2.1.4.2 *Hydrogen bonding*

Hydrogen bonds are formed between the oxygen or hydroxyl of the clay surface and the adsorbed molecule. Hydrogen bonding becomes significant especially in large molecules or polymers as a high molecular weight of the polymer tend to result in more hydrogen bonds and a relatively stable complex. However, for small molecules such as water and glycerol, hydrogen bonding only causes weak attraction and in this case ion-dipole interactions dominate. Moreover, hydrogen bonding through the water bridge mechanism is often a much more significant interaction when combining polar organic molecules to clay surfaces.²⁷

2.1.4.3 *Van der Waals force*

Van der Waals forces work between all atoms, ions and molecules, but it's relatively weak. It's caused by the attraction between oscillating dipoles in adjacent atoms and its influence decreases rapidly with the increasing distance between the interacting species. In the system containing polymers, this attractive force becomes quite important due to large molecular weights.²⁷

2.1.4.4 *Hydrophobic interaction*

In aqueous solutions, the attractive interaction between organic nonpolar molecules, e.g. hydrocarbons, is very strong. This 'hydrophobic interaction' is the reason for the low solubility of hydrophobic molecules in water, and plays an important role in micelle formation, biological membrane structure, and is responsible for the conformations of proteins. It is a long-range interaction that involves the rearrangement of water molecules as two hydrophobic species come together.²⁸

2.1.4.5 *Steric interaction*

Steric interaction can occur in colloidal systems with grafted or adsorbed polymer strands that protrude from the colloidal surface. Two particles will repel each other when their respective polymer strands start to entangle due to the entropy decrease of the polymer strands.²⁹ The steric stabilization is an important and robust way to stabilize colloidal dispersions that can be relative insensitivity to the salt and pH changes.¹⁰

2.1.5 *Colloid stability*

In any stable colloidal dispersion, the overall interaction between the particles is repulsive. When the stability of the dispersions is disturbed the particles eventually flocculate or aggregate and gel. The formation of aggregated particle networks has strong effects on the rheological properties of the clay dispersions. Generally, stable colloidal dispersions show liquid-like behaviour with shear thinning or thickening character, while the plastic character often appear together with thixotropy due to the network formation of aggregated particles.¹³

The stability of a dispersion is governed by the particle interactions. Particles interactions and aggregation have strong effects of the physical properties of colloidal dispersions. Van der Waals and electrostatic interactions are common forces that cause aggregation.⁹ To counteract the Van

der Waals forces and promote the stability, equally long-range repulsive forces are required. Grafted charged chemical groups, polymer or surfactant additives are often used as stabilizers in colloidal dispersions.³⁰

Colloidal stability can also be affected by factors such as shape and size of the particles, pH and salt concentration. Nontronite particles have a sheet or plate morphology and such anisotropic particles are known to form nematic liquid crystals. Because of the large anisotropy of the clay plates, they effectively occupy a much larger volume than the clay plate in itself. Therefore the nontronite dispersion gel at low solid concentrations.³¹ The stability of colloidal nontronite dispersions is also influenced by pH. The clay plates in dispersion have negatively charged faces, while their edges are conditionally charged. This means that the edges are positively charged at pH values lower than the isoelectric point (*IEP*) and negative at pH values higher than the *IEP*. When the edges of clay plates are neutral, the pH of the dispersion is at its *IEP*.³² The salt concentration can also change the stability of a colloidal dispersion. As mentioned in section 2.1.1.2, nontronite has different phase behaviours depending on the salt concentration.

2.1.5.1 *DLVO theory*

The interactions between particles in colloidal systems can be interpreted by Derjaguin-Landau-Verwey-Overbeek (DLVO) theory. According to this theory, the stability of colloidal dispersions is dependent on the balance between the van der Waals force and the electrostatic interaction between colloidal particles.³³ For example, the relatively large van der Waals force of the electron rich clay plates causes an attractive force between clay plates while the electrostatic interaction between the negative faces and positively charged edges of the clay plates results in both repulsion and attraction.

2.1.5.2 *Gelation*

One definition of gelation says that if all of the solvent is mechanically immobilised within an aggregates network and the whole system presents a solid appearance, it is a gel.⁹ Colloidal gels are typically formed by particle aggregation and the rigidity of the gel depends on the particle concentration and the strength and number of the links between the particles.

The mechanism of clay gel formation is still debated but two main mechanisms have been proposed.^{34, 35} One is the “house of cards” model. The model assumes that the interactions between charged edges (+) and faces (-) induced by electrostatic attractions dominate at low-moderate salt concentration and acidic condition. At moderate to high salt concentration, “zig-zag” ribbons or band-like structures are induced by edge-edge and face-face interactions. The second model states that gelation is caused by repulsive forces between the interacting electric double layers of the plates, forming repulsive gels.

2.2 Birefringence

Optical birefringence is defined as the difference between the maximum and minimum refractive index values.³⁶ When light enters an isotropic crystal, it's refracted at a constant angle and passes through the crystal at a single velocity without being polarized by the crystalline lattice. However, anisotropic crystals have crystallographically distinct axes and interact with light which depends on the orientation of the crystalline lattice. When light enters a non-equivalent axis, it is refracted into two rays each polarized with various directions and velocities, this is called double refraction. Birefringence (B) is responsible for the phenomenon of double refraction and is formulated as:

$$B = |n_{high} - n_{low}| \quad (1)$$

Here n_{low} is the smallest refractive index and n_{high} is the largest.³⁷

The birefringent behaviour of anisotropic crystals can be examined under a polarizing microscope. If the isotropic samples are placed in crossed polarizers, they appear dark. An anisotropic crystal on the other hand, display stronger birefringence brightness the more aligned the sample is.

3 Materials and Methods

3.1 Materials

In this study two sources of nontronite clay were used. One was purchased from Excalibur Mineral Corp, Peekskill, NY, and the clay had been mined in Allentown, Pennsylvania, USA. The second nontronite was purchased from Source Clays Minerals repository West Lafayette, Indiana, USA and the clay had been mined at Uley Graphite Mine, South Australia, Australia. These will from now on be referred to as Nam (Nontronite-USA) and NAu (Nontronite-Australia). Both NAm and NAu dispersions were prepared by following a protocol previously used by Abrahamsson and colleagues². In short, 3 g of nontronite was ground and dispersed in 1 M NaCl (Sigma-Aldrich, Sweden) followed by ultra-sonication (Processor VC505, Sonics Newtown, CT, USA). The dispersion was centrifuged (Optima XL-100K ultracentrifuge with 90 Ti rotor, Beckman Coulter, Palo Alto, CA, USA) at 35000×g for 90 min and re-dispersed into NaCl solution in total 3 times to exchange all ions to sodium ions. The sediment from the last centrifugation was dispersed in 210 ml deionized water and was dialysed against deionized water until no change in conductivity was observed. The exchanged nontronite dispersion was size fractionated by centrifugation at 7000×g to get size fraction 1 dispersion and at 17000×g to get size fraction 2 dispersion. All experiments were done using the clay sediment from size fraction 2 (s2). In the case of NAm s2, the dispersion was dialysed against 10^{-4} M NaCl solution for one week to achieve a constant salt concentration in all samples.

The glycerol (99.5%) used in this investigation was purchased from Sigma-Aldrich. Sodium chloride was added to the glycerol to get a salt concentration of 10^{-4} M NaCl. The PMAAm used had a \overline{M}_N of 28000 and was kindly synthesised and provided by Katherine Locock (CSIRO Material Science and Engineering, Clayton, Australia) using RAFT polymerisation and its structure is shown in Figure 6. The UCST of the polymer solution was visually observed by eye and was estimated to be around 50 °C.

3.2 Sample formulation and phase diagrams

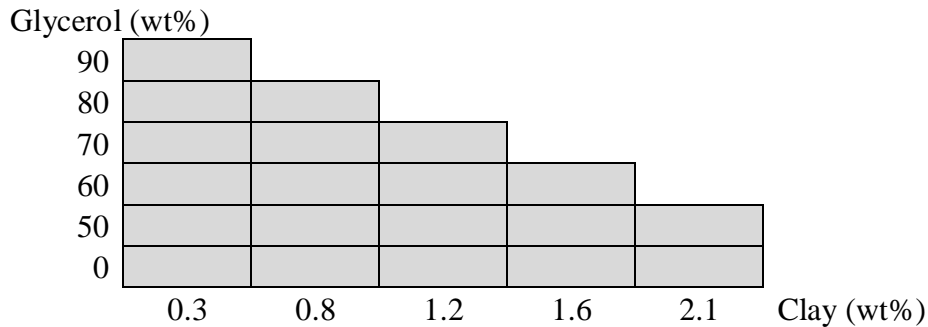


Table 1 Plan for a phase diagram investigation with samples of different NAm s2 clay and glycerol concentration.

To investigate the effect of clay and glycerol concentration a plan (see Table 1) consisting of 20 samples was devised. From Table 1 we can see that the clay concentration spans between 0.3 to 2.1 wt%, and the glycerol concentration in water is between 0 and 90 wt%. The plan for the phase diagram investigation is a triangle-shaped as the clay concentration of NAm s2 dispersion could not be made high enough to prepare samples with both high clay and high glycerol concentration.

Briefly, these samples were prepared in several steps. To ensure a constant salt concentration in all samples, all sample constituent liquids (NAu s2 dispersion, glycerol and water) was set to have a NaCl concentration of 10^{-4} M. After adding all components to a 1.5 ml Eppendorf tube the tube was vortexed. Vortexing time depended on the viscosity of the samples, and vortexing was continued until the sample was well dispersed as judged by eye. The samples were then transferred into 2 ml glass vials (ID 12 mm, L 32 mm; Bellefonte, PA, USA) with plastic screw caps or NMR tubes (Type 5TA, OD 5 mm, ID 4 mm, L 178 mm; Döttingen, Switzerland) depending on the experiment. The pH of each sample was tested using pH meter (744 pH meter, Metrohm, Switzerland).

PMAAm (wt%)			
3			
2.5			
2			
1.5			
1			
0.5			
0			
	1.5	2.1	2.4
	clay (wt%)		

Table 2 Plan for phase diagram investigation with samples of different NAu s2 clay and PMAAm concentration.

In case of the NAu s2 clay-PMAAm system, the pure PMAAm dispersions' properties were investigated first. Samples with 1 and 3 wt% polymer were prepared by alternately heating (up to 75 °C) and vortexing until the samples were well dispersed. Overheating was avoided as this could cause degradation of the polymer. The samples were imaged between crossed polarizers at 25 °C and 75 °C. Afterwards, both of them were left undisturbed for several days and phase separation was imaged at 2 and 5 days.

Table 2 shows a plan with 21 samples with a clay concentration between 1.5 to 2.4 wt% and a PMAAm concentration between 0 to 3 wt%. All samples were prepared in 1.5 ml Eppendorf according to Table 2. Then all samples were heated in 75 °C water bath for 2 min and vortexed for 1 min and this step was repeated 3 times. Then samples were reheated and transferred into square glass tubes (ID 3mm, L 48mm, VitroCom, UK). In total all samples experienced less than 10 min heating to avoid degradation of the polymer due to hydrolysis.

3.3 Observations of samples between crossed polarizers

The purpose of the birefringence test was to check for aligned clay particle regions by observing the samples between crossed polarizers. Samples in Table 1 were observed between the polarizers before and after shaking or before and after exposure to the magnetic field. The light source laptop computer screen set to have a white desktop background. This light source produced a homogenous white light suitable for observation of samples between crossed polarisers. Polarizers were integrated with a cardboard box to hinder any unpolarised light from entering the box. To observe the relaxation time of the flow birefringence in the samples, the samples were imaged between crossed polarizers directly after shaking, the sample was then left undisturbed and imaged after 5 days. The procedure of observation between crossed polarizer before/after magnetization was as follows. Firstly, the samples were transferred into NMR tubes and imaged before magnetization. Secondly, the NMR tubes were inserted into NMR magnet for 2 min and the samples were then imaged outside the NMR magnet within 1 min. The intensity of magnet was 14 T. In all photos the NMR tubes with samples were leaning 45° relative the horizontal plane. Two phase diagrams were made, one at which the salt concentration was kept constant at 10^{-4} M NaCl (Figure 9) while the second had no added salt (Figure 10).

For the clay-PMAAm dispersions, all samples in Table 2 were shaken, vortexed and imaged between crossed-polarizers before magnetization. Next, samples were placed into NMR magnet at 75 °C. The temperature increased from 25 °C to 75 °C in 2 min and was kept there for 5 min. Then temperature decreased to 25 °C in 10 min. Hence the total time of magnetic field exposure for the samples was 17 min and samples were imaged between crossed-polarizers after this. Then samples were shaken and vortexed samples again and exposed to magnetic field at 25 °C for 17 min and imaged between crossed polarizers.

3.4 Rheological observations with inverted tube test

To understand the clay dynamics of the different samples macro and micro-rheological measurements were performed. A quick macro-rheological test, called an “inverted tube test” was performed in which the tube with the sample was inverted upside down and gently shaken. If the sample flowed it was considered to be a liquid, if not it was defined as a gel.

Four states of rheology were defined in the inverted tube test including liquid, liquid-gel, gel and mechanical unstable gel. Liquid-gel means the sample flowed very slowly when inverted and mechanical unstable gel means the sample did not flow at first but when sufficient shaking was applied the dispersion/gel flowed down quickly.

3.5 Protocol of rheological measurement with rheometer

The aim of measuring the rheological properties of clay-glycerol samples (according to Table 1) was to investigate the macro-viscosity of clay-glycerol dispersions and to compare these results

to the micro-rheology measurements represented by the magnetic alignment and relaxation observations made between crossed polarizers.

A Physica MCR 300 rheometer was used for measurements with a small cone and plate geometry whose diameter is 50 mm and angle is 1°. A moisture device was installed to avoid evaporation of samples. Details of rheometer setting are shown in Table 3. In the beginning, temperature was set at 25 °C and tested sample was rested for 5 min. Then a gentle oscillation amplitude sweep was applied with strain is 1% and frequency is 1 Hz. After this, the storage and loss modulus were measured again in an oscillation amplitude sweep using strain range from 0.01% to 10%. From this step, γ_0 could be found in constant region of G' and G'' where both storage and loss modulus are stable. Next, an oscillation frequency sweep was performed with controlled strain γ_0 and frequencies of between 0.005 Hz and 30 Hz. In the end, ascending and descending flow curves were then recorded twice, viscosity changes of samples could be tested under controlled shear rate increasing from 0.1 to 1000 s⁻¹ then decreasing. The viscosity of the samples were transformed to relative viscosity by the equation:

$$\eta_r = \frac{\eta_s}{\eta_g} \quad (2)$$

Where η_s is viscosity of the sample tested by the rheometer, η_g is the viscosity of aqueous glycerol solution which has same glycerol concentration with the sample at 25 °C, η_r is the relative viscosity.

Stage	Step	Parameters
1	Resting	Set T = 25 °C t = 5 min
2	Oscillation amplitude sweep with set time	$\gamma = 1\%$ $\nu = 1 \text{ Hz}$ t = 10 s/pt, 60 points
3	Oscillation amplitude sweep with controlled frequency	$\gamma = 0.01 \text{ to } 10\%$ $\nu = 1 \text{ Hz}$ No time setting, 60 points
4	Oscillation frequency sweep	$\gamma_0 = \text{See "Note"}$ $\nu = 0.005 \text{ to } 30 \text{ Hz}$ No time setting, 60 points
5	Ascending flow curve (1)	$\dot{\gamma} = 0.1 \text{ to } 1000 \text{ s}^{-1}$ t = 10 s/pt, 40 points
6	Descending flow curve (1)	$\dot{\gamma} = 1000 \text{ to } 0.1 \text{ s}^{-1}$ t = 10 s/pt, 40 points
7	Ascending flow curve (2)	$\dot{\gamma} = 0.1 \text{ to } 1000 \text{ s}^{-1}$ t = 10 s/pt, 40 points
8	Descending flow curve (2)	$\dot{\gamma} = 1000 \text{ to } 0.1 \text{ s}^{-1}$ t = 10 s/pt, 40 points

Table 3 Rheometer test procedure on NAm s2 clay-glycerol dispersions. Note: A suitable γ_0 was chosen by aiming for an as large amplitude as possible from step 3 where G' and G'' remain at a constant level.

3.6 Investigating relaxation of clay particles

The relaxation of the oriented regions of the samples was investigated by measuring the light intensity of birefringence over time by using a Nikon D3200, Nikon Corp with a Nikon AF-S 40 mm f/2.8 G objective and image analysis with the software ImageJ. To increase the mixing of the samples, four (Φ 1.5 mm \times 3 mm) stainless steel bars was added to each vial after which the samples were shaken for 30 seconds by hand. The samples were then imaged over time between crossed polarizers with a device which was same with the one in section 3.3. The samples highlighted with blue colour in Table 4 proved to have relaxation times appropriate for the measurement method. The samples with lower clay concentration relaxed immediately while the samples with higher clay concentration did not relax within the experimental time frame.

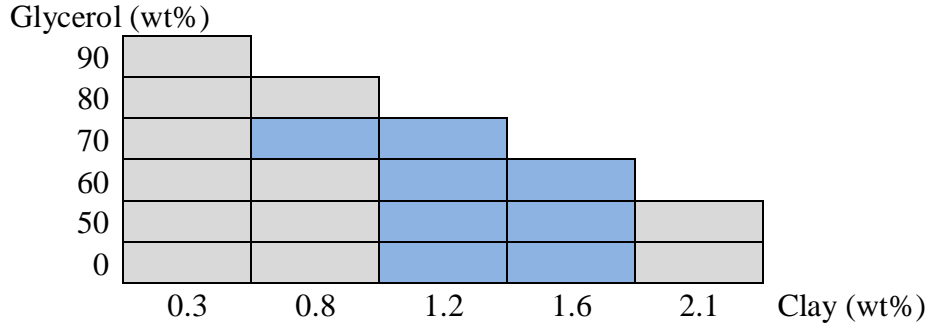


Table 4 NAm s2 clay-glycerol samples (highlighted in blue) were selected for monitoring the relaxation process.

During the relaxation process of clay-glycerol samples, images were taken with suitable intervals adjusting for their individual relaxation time. Afterwards, 20 photos were chosen to analyse the light intensity I_i by ImageJ. Final relative intensity I_{ri} is calculated as below:

$$I_{ri} = \frac{I_i - I_b}{I_1 - I_b} \quad (i = 1, 2, 3 \dots 20) \quad (3)$$

Where I_b is background intensity estimated by curve-fitting using Origin, I_1 is initial intensity which means the highest intensity measured after shaking step. In the end, I_{ri} was plotted as a function of time and fitted relaxation curves could be received according to:

$$I_{ri} = A_1 e^{\left(-\frac{x}{t_1}\right)} + y_0 \quad (4)$$

Where t_1 is relaxation time which is exponential to relative intensity I_{ri} , x is time and A_1 and y_0 are constants.

4 Results

4.1 Colloidal system consisting of NAm s2 clay and aqueous glycerol solution

The following results are from observations of NAm s2 clay-glycerol dispersions. The investigated samples are according to the phase diagram plan shown in Table 1. For clarity, it's important to mention that the salt concentration in the samples in Table 5 and Figure 10 was not set to 10^{-4} M NaCl as they are results that are presented later in this thesis. These experiments include observation of birefringence (section 4.2, except Figure 10), pH (section 4.3), rheology (section 4.4) and relaxation time (section 4.5).

4.1.1 *Inverted tube test*

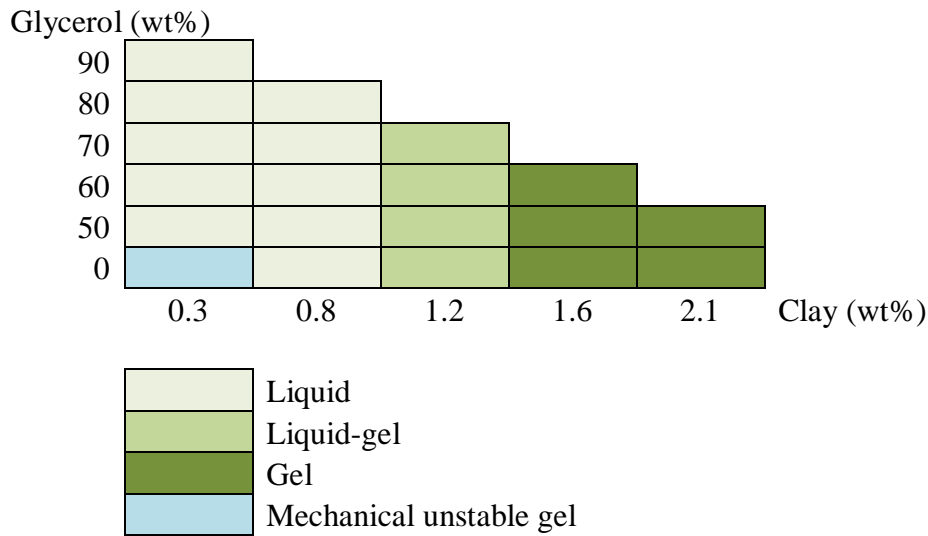


Table 5 Schematic graph for inverted tube test results (no set constant salt concentration in samples).

Table 5 shows the macro-viscosity of the samples as judged by the inverted tube test. The samples appeared more viscous with increasing clay concentration and the samples with a clay concentration of 1.6 wt% and 2.1 wt% clay were gels. Samples with 1.2 wt% clay were liquid-gels, which means that the dispersions could flow very slowly after the tubes were inverted. Moreover, at dilute clay concentration (<1.2 wt%) the samples were liquid and flowed down immediately. However, sample R1 containing 0.3 wt% clay and 0 wt% glycerol was a noteworthy exception. After the tube containing sample R1 was inverted, the dispersion did not flow down, but after gentle shaking it flowed immediately and this was defined as a 'mechanical unstable gel'. From Table 5 it appears like the rheological behaviour of the samples was dominated by the amount of clay and not so much by the addition of glycerol.

4.1.2 *Observation of birefringence*

The presence of birefringence in Figure 7-10 indicates regions where the clays were locally or collectively aligned.

4.1.2.1 *Random observation*

Figure 7 shows that the samples with 1.6 and 2.1 wt% clay were strongly birefringent directly after shaking the samples, and the samples with 1.2 wt% clay showed a slight birefringence that relaxed relatively fast compared to a higher clay concentration. Samples with only 0.3 wt% and 0.8 wt% clay were dark and did not show any birefringence. It's obvious that the clay concentration was the main factor controlling the intensity of birefringence.

In the 1.2 wt% clay samples and with increasing glycerol concentration, the birefringence decreased in the 50 wt% glycerol sample compared with the clay-water sample (no glycerol), but then increased from 50 to 70 wt% of glycerol. At a glycerol concentration of 80% and 90% the samples were well dispersed as judged by eye directly after preparing the samples. However, some of the clay particles in these samples aggregated and formed a dense sediment within a day or two. In Figure 7 the suspended aggregates in the samples with 80 and 90 wt% glycerol are visible and the dense sediment they formed after 5 days can be seen in Figure 8. The aggregates in the sample with 0.8 wt% clay and 80 wt% glycerol were still suspended in the whole liquid volume, probably because of the reduced sedimentation speed at a clay concentration of 0.8 wt% compared to 0.3 wt%.

Figure 8 shows the samples after being undisturbed for 5 days and many of these samples lost their birefringence after 5 days compared to directly after shaking. Interestingly, the sample with 1.6 wt% of clay and 0 wt% of glycerol was still birefringent, but the birefringence disappeared in the samples with same clay concentration and higher glycerol concentration.

4.1.2.2 *Observation of samples before and after magnetization*

Figure 9 (left) shows the phase diagram imaged between crossed polarizers before magnetization. All samples compositions in the NMR tubes had the same behaviour as the undisturbed solutions in 2ml vials in Figure 8. In samples of 1.6 wt% pure clay dispersion the bottom part of the sample had a stronger birefringence than the top part. This is because the top part of the sample was more sensitive to the movement of the liquid as the samples were transported between the NMR magnet and the birefringence visualization set-up. The comparably larger mechanical disturbances of the top part of the sample increased the speed of the birefringence relaxation.

Figure 9 (right) shows the phase diagram after magnetization, where samples with 0.3 and 0.8 wt% clay were dark and did not show any birefringence, just as before magnetic exposure. The samples with 1.2 and 1.6 wt% of clay on the other hand appeared to be fully aligned by the magnetic field. Samples with 2.1 wt% of clay did get a slightly stronger birefringence, but the alignment of the samples was not homogenous as the nematic-like patterns were not aligned in one direction. Hence the sample alignment was unlikely to have gone to completion at this clay concentration. Moreover, the bottom part of the 1.2 and 1.6 wt% pure clay samples was more colourful than the top parts. Similar with the results in Figure 7, the birefringent colours are

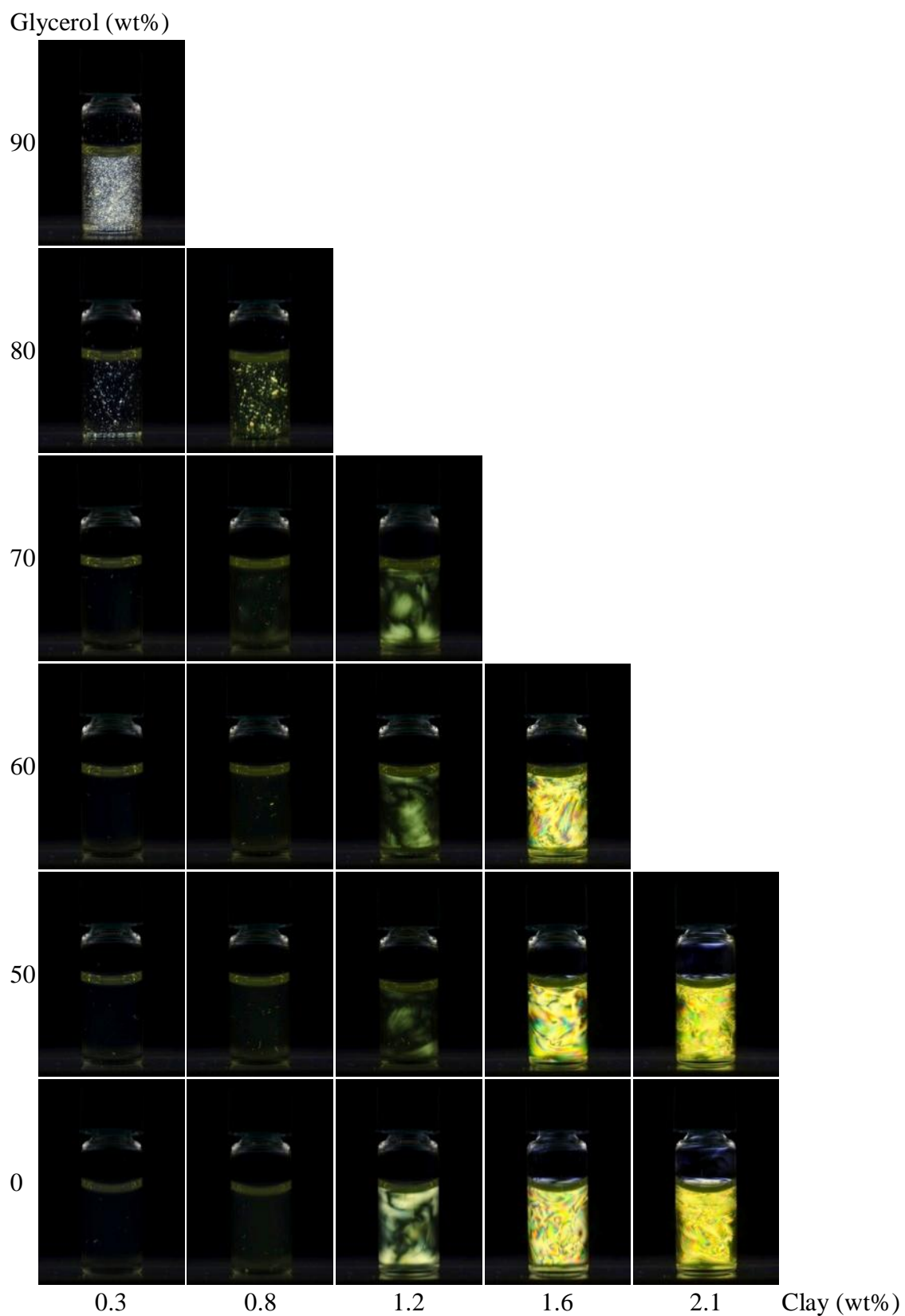


Figure 7 NAm s2 clay-glycerol dispersions imaged between crossed polarizers directly after shaking. The salt concentration in all samples was set to 10^{-4} M NaCl.



Figure 8 NAM s2 clay-glycerol dispersions imaged between crossed polarizers after being left undisturbed for 5 days. The salt concentration in all samples was set to 10^{-4} M NaCl.

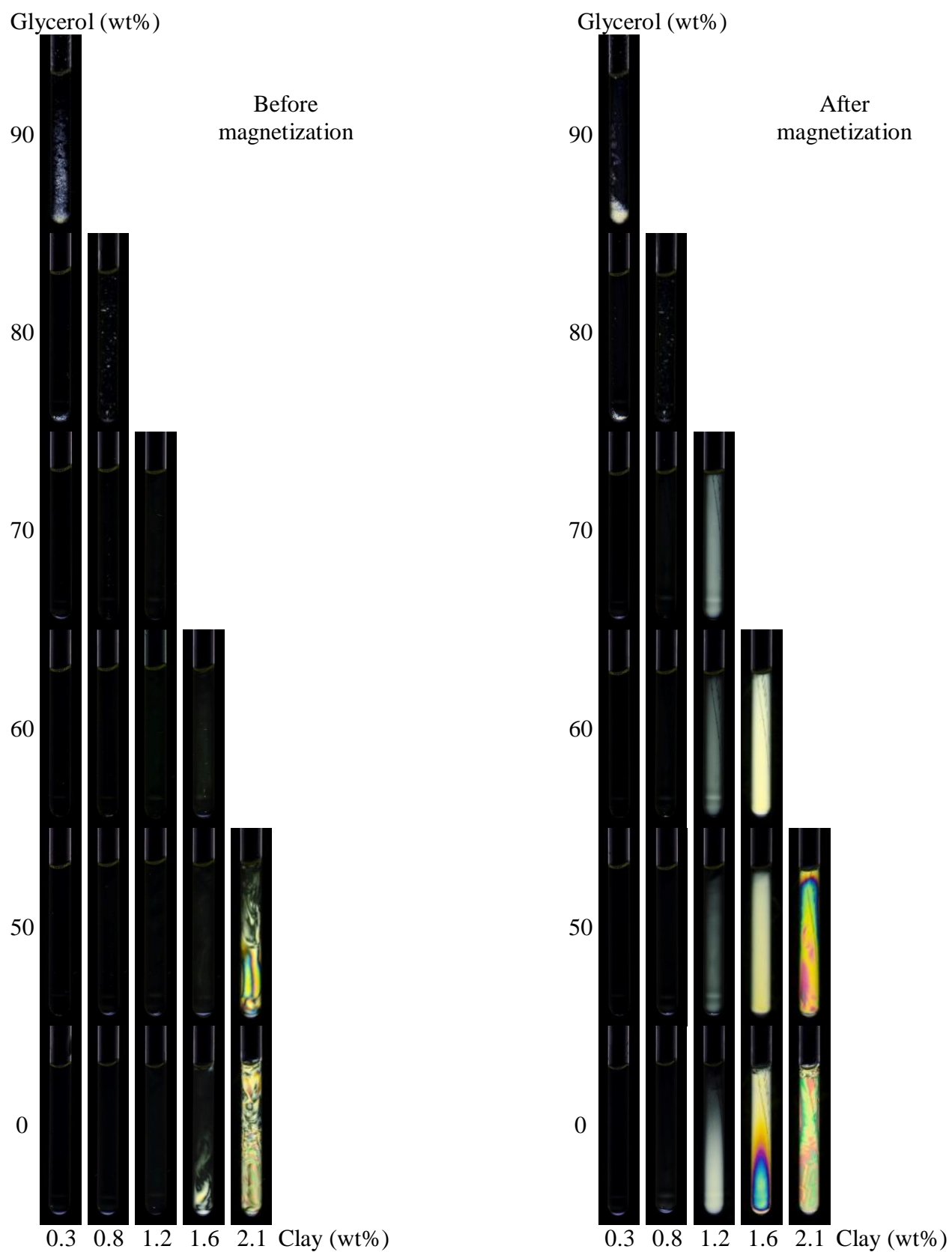


Figure 9 NAm s2 clay-glycerol dispersions imaged between crossed polarizers before (left) and after (right) magnetization. The salt concentration was set to 10^{-4} M NaCl.

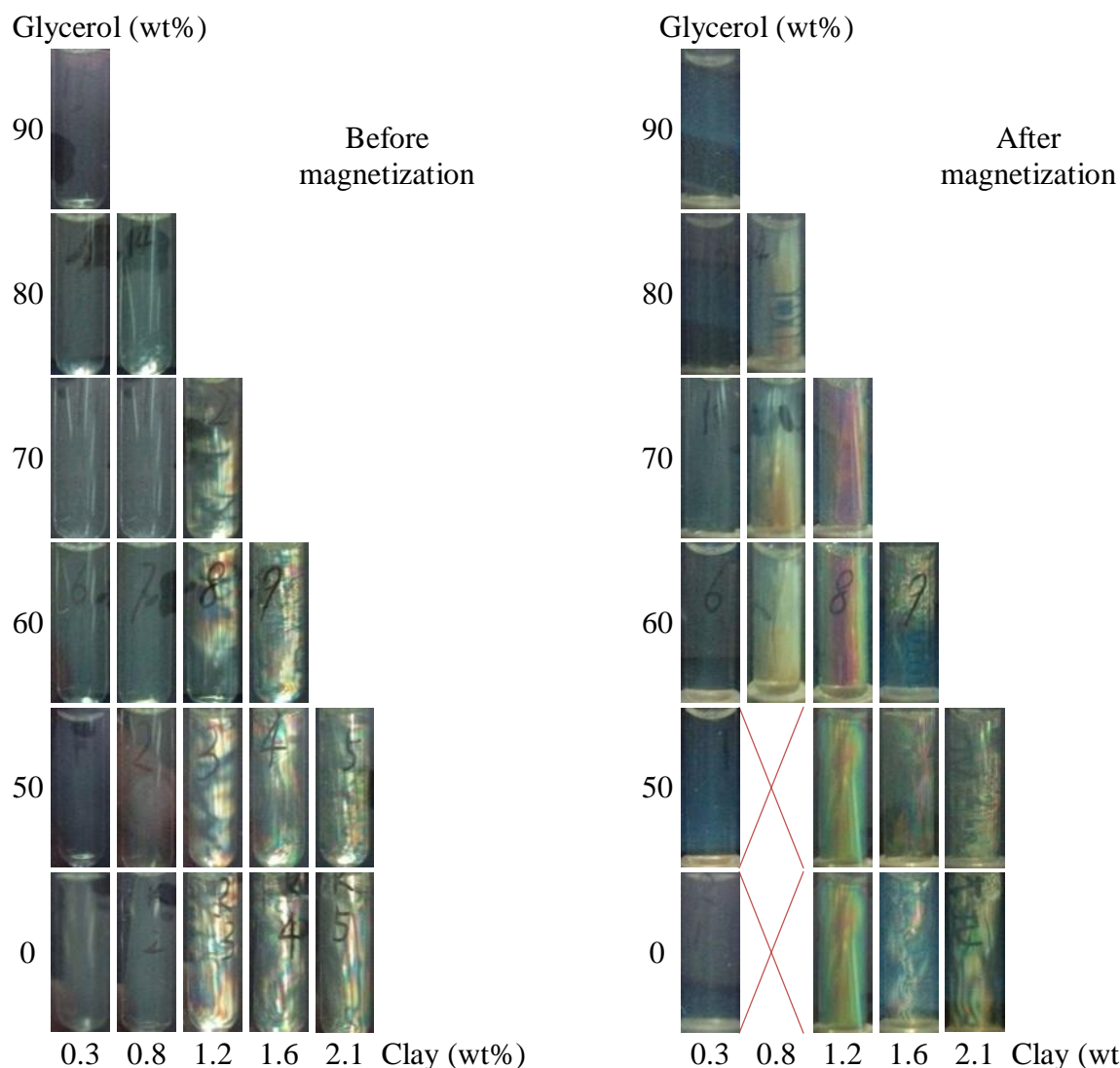


Figure 10 NAM s2 clay-glycerol dispersions imaged between crossed polarizers before (left) and after (right) magnetization. No salt was added to the samples. Imaging of the samples with 0.8 wt% clay and with no glycerol and 50 wt% glycerol on the right failed and are hence not available.

brighter in the sample of 1.2 wt% pure clay dispersion compared to those samples with same clay concentration but with glycerol.

In Figure 10 the phase diagrams without a set salt concentration are shown before and after magnetic exposure. These samples were same samples used for the inverted tube test in Table 5. The birefringence phase behaviours in the samples without added salt were very different from the ones with a set salt concentration (10^{-4} M NaCl). Overall there were more samples that were birefringent when no salt was added as illustrated in the right phase diagram in Figure 10, where the magnetically exposed samples with 0.8 wt% clay showed birefringence. However, the equivalent samples with added salt in Figure 9 (right) showed no birefringence.

4.1.3 Clay dispersion pH

The pH values of samples for the phase diagram investigation shown in Table 1 were measured with a pH meter and the results are illustrated in Figure 11. With increasing clay concentration the pH of the samples was reduced. Furthermore, the addition of glycerol lowered the pH but this effect levelled off at the higher glycerol concentrations tested.

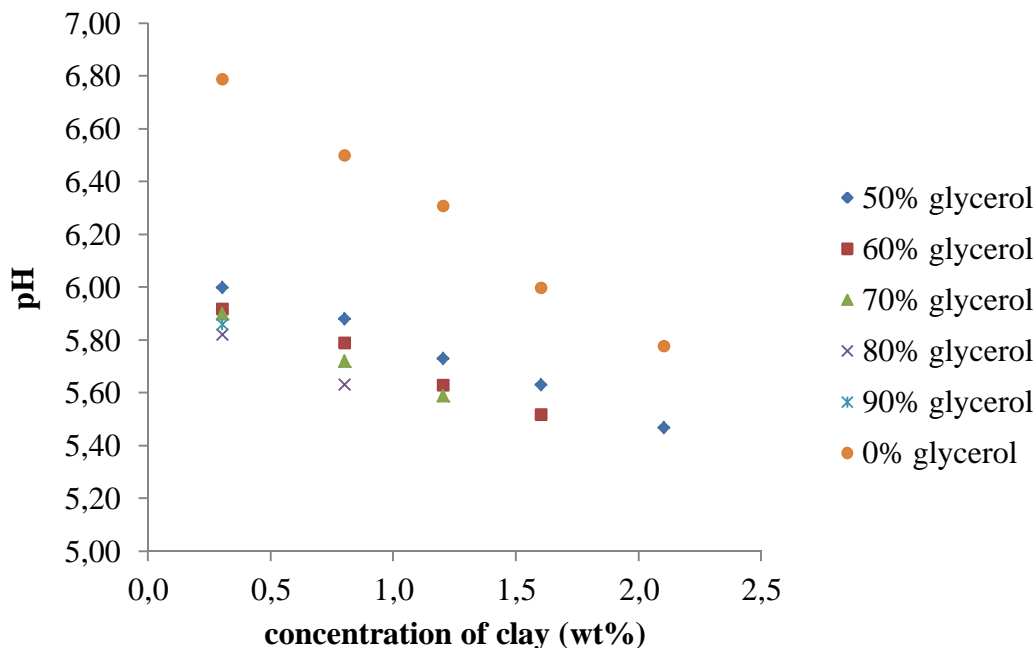


Figure 11 pH of NAM s2 clay-glycerol dispersions in phase diagram

4.1.4 Rheology characterization

The macro-rheological properties of the NAM s2 clay-glycerol dispersions in the phase diagram (Table 1) were characterized by oscillation frequency sweeps and steady-state flow curves with the rheometer.

From frequency sweep graphs (Figure 12, 15 and 18), it can be seen that with increasing frequency, the storage (G') and loss modulus (G'') of most of samples increased before reaching a plateau, but some samples had a drop in the beginning of the sweeps. In the end, G' and G'' grew again. The G' and G'' in plateau regions were considered as the 'real' storage and loss modulus of materials. For comparison of storage and loss modulus of each sample, values of G' and G'' at 0.11 Hz in Figure 12, 15 and 18 were chosen to be representatives and plotted in Figure 14, 17 and 20.

In steady-state flow curves in Figure 13, 16 and 19 we can see that the relative viscosities of all samples first declined with increasing shear rate and then increased again with decreasing shear

rate. Similar with frequency sweeps, values of the relative viscosity at 1.06 s^{-1} were compared and plotted in Figure 14, 17 and 20.

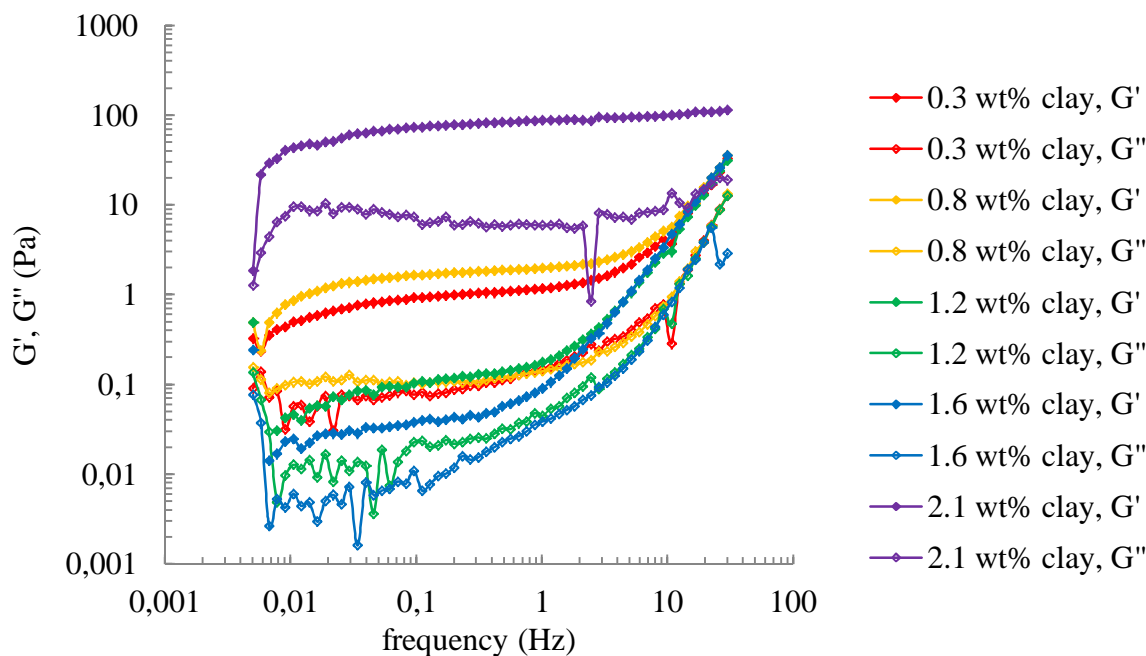


Figure 12 Frequency sweep for samples with no glycerol and different clay concentrations, the range of frequency is from 0.5 Hz to 30 Hz.

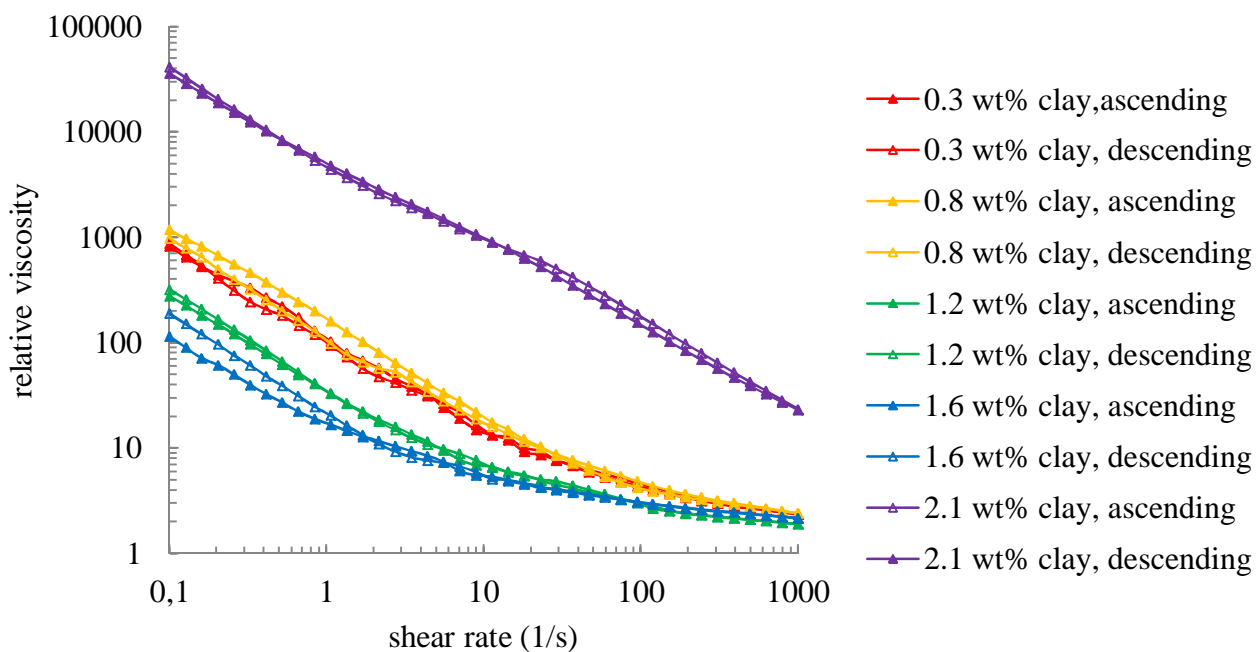


Figure 13 Second time ascending and descending flows for samples with no glycerol and different clay concentrations, the shear rate is from 0.1 to 1000 s^{-1} .

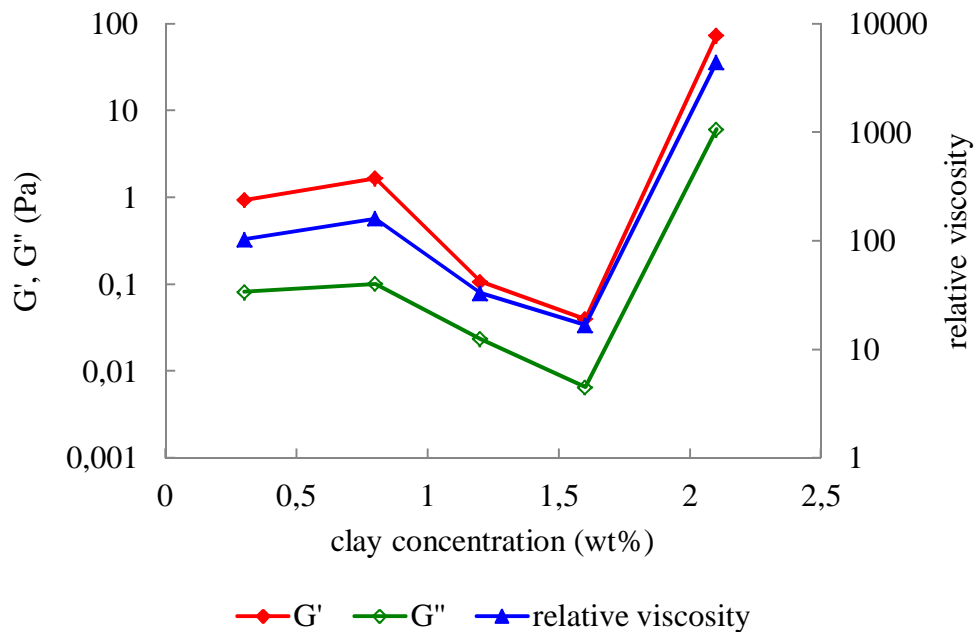


Figure 14 G' , G'' and relative viscosity of samples with no glycerol versus clay concentration. The G' and G'' values were taken at 0.11 Hz from Figure 12. The relative viscosity values were taken at 1.06 s^{-1} from Figure 13.

Figure 14 shows that for pure clay dispersions the relative viscosity, G' and G'' increased slightly between 0.3 and 0.8 wt% clay, followed by a drop to a minimum in going from 0.8 to 1.6 wt%. These properties then increased steeply between 1.6 and 2.1 wt%.

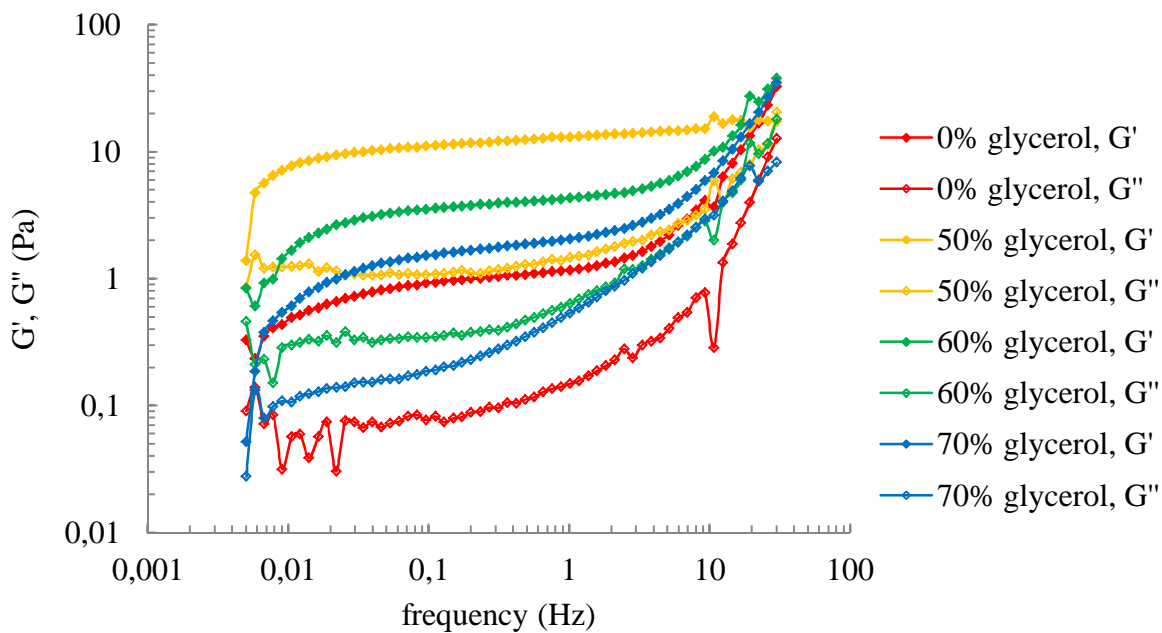


Figure 15 Frequency sweep for samples with 0.3 wt% clay and different glycerol concentrations.

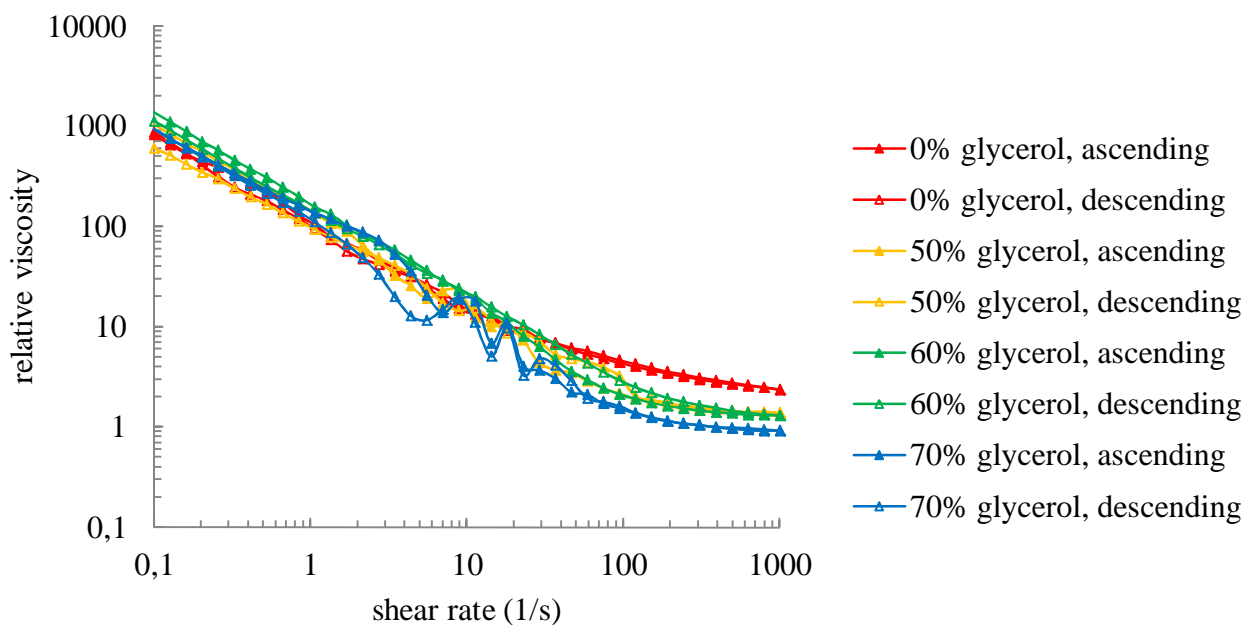


Figure 16 Ascending and descending flows curves for samples with 0.3 wt% clay and different glycerol concentrations.

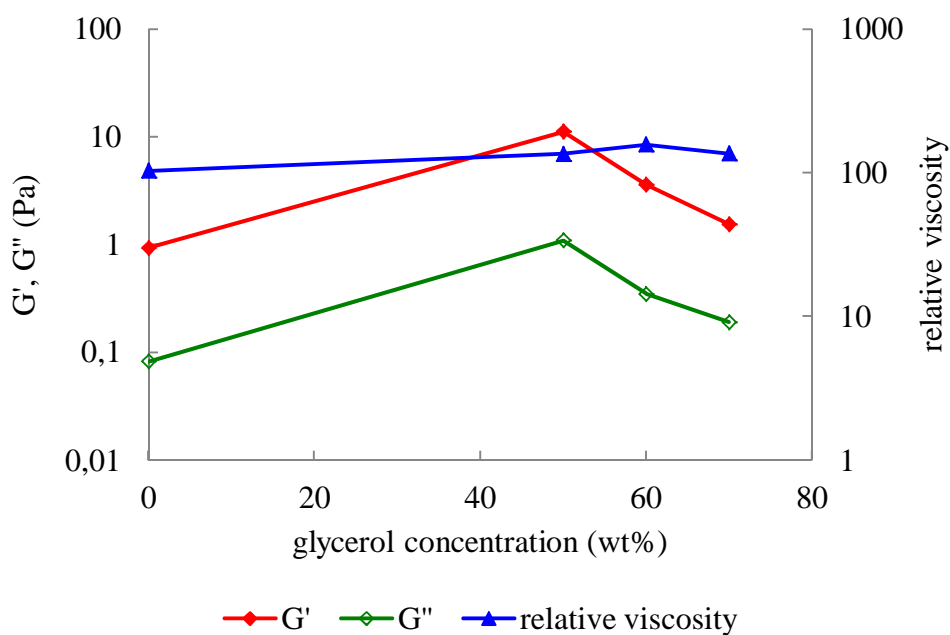


Figure 17 G' , G'' and relative viscosity of samples with 0.3 wt% clay versus glycerol concentration. The values of G' and G'' were taken at 0.11 Hz from Figure 15. The values of relative viscosity were obtained at $1.06 s^{-1}$ from Figure 16.

A comparison between samples with 0.3 wt% of clay and different glycerol concentrations were made in Figure 17. As glycerol concentration was increased, the G' and G'' first increased and then decreased. The relative viscosity, however, remained constant at all glycerol concentrations.

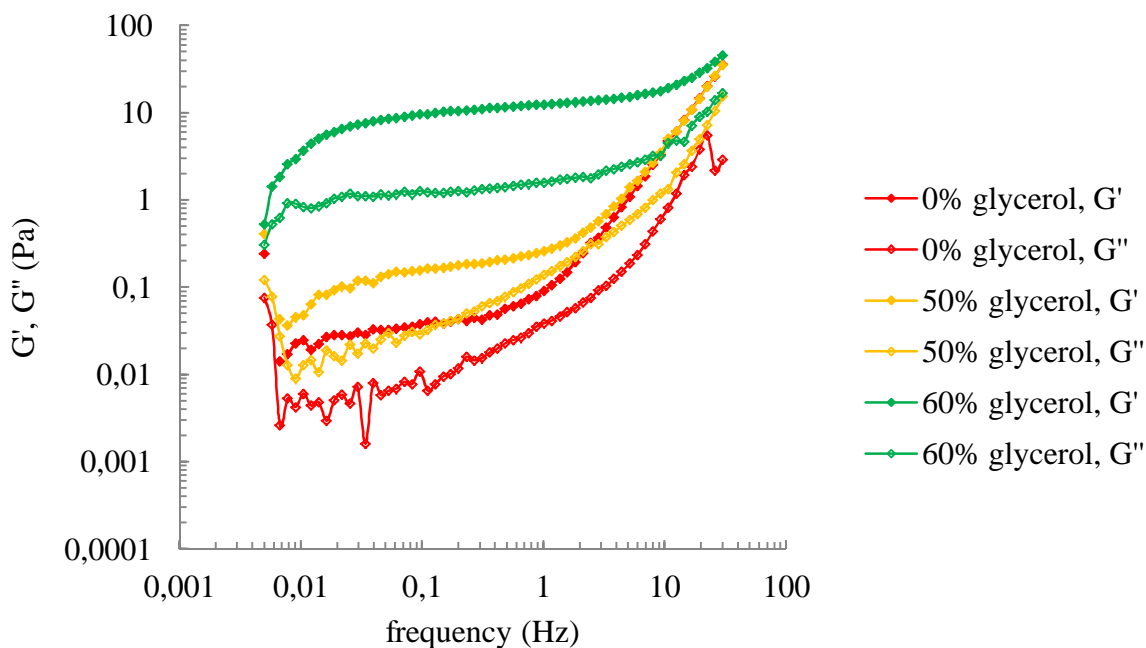


Figure 18 Frequency sweep for samples with 1.6 wt% clay and different glycerol concentrations, the range of frequency is from 0.5 Hz to 30 Hz.

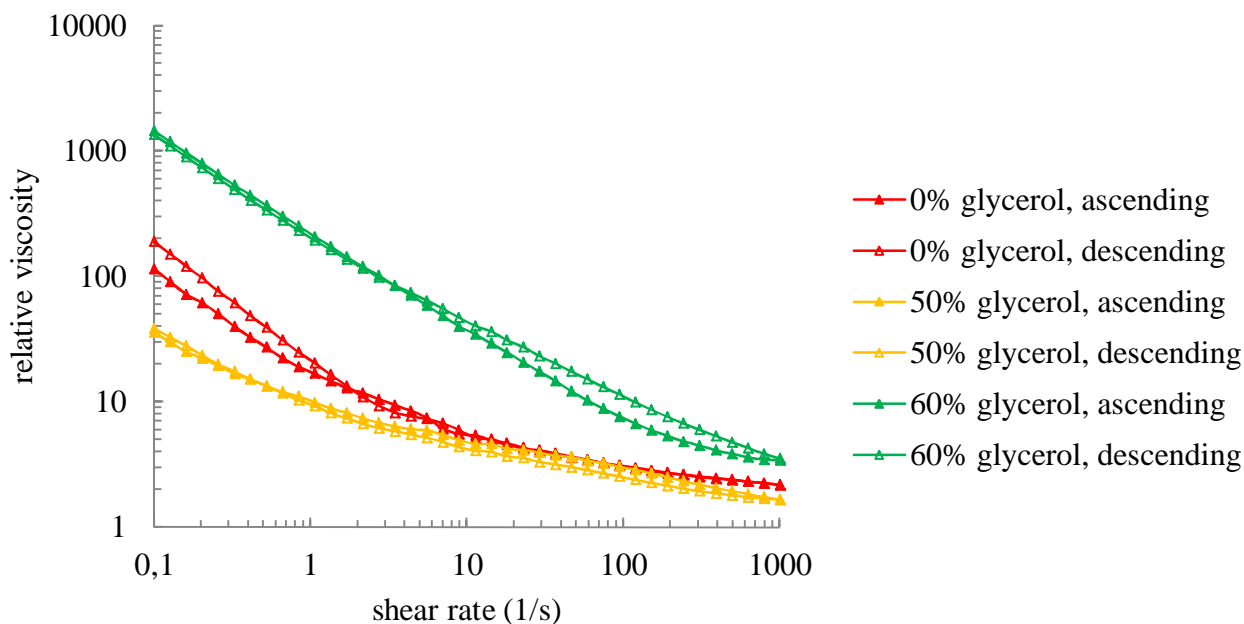


Figure 19 Ascending and descending flows curves for samples with 1.6 wt% clay and different glycerol concentrations.

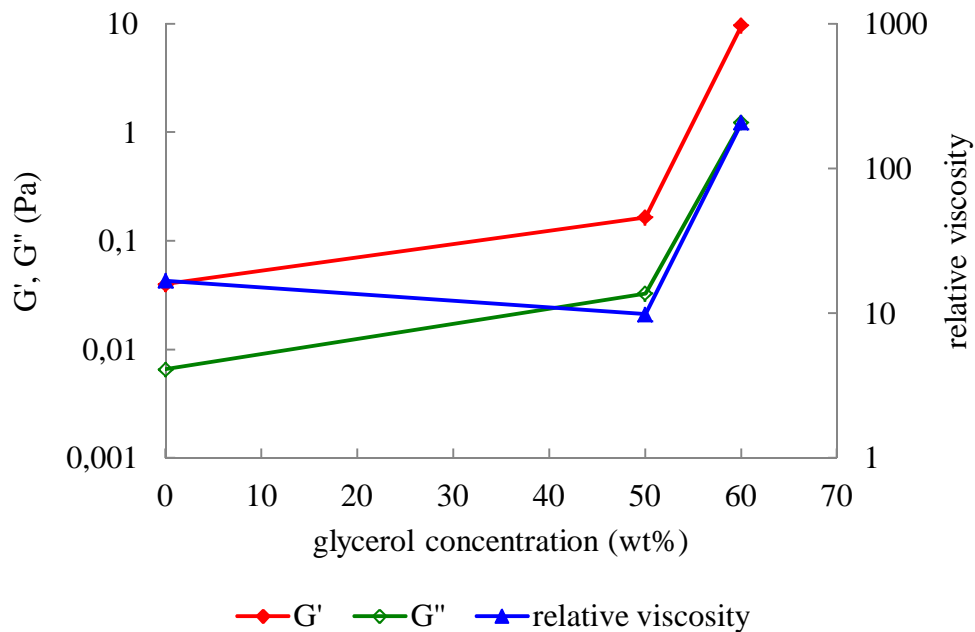


Figure 20 G' , G'' and relative viscosity of 1.6 wt% clay dispersions versus glycerol concentration. The values of G' and G'' were taken at 0.11 Hz from Figure 18. The values of relative viscosity were obtained at 1.06 s^{-1} from Figure 19.

The G' , G'' and relative viscosity of samples with a clay concentration of 1.6 wt% are shown in Figure 20. G' and G'' increased as glycerol concentration was increased, while the relative viscosity declined slightly and then increased.

4.1.5 Relaxation measurements

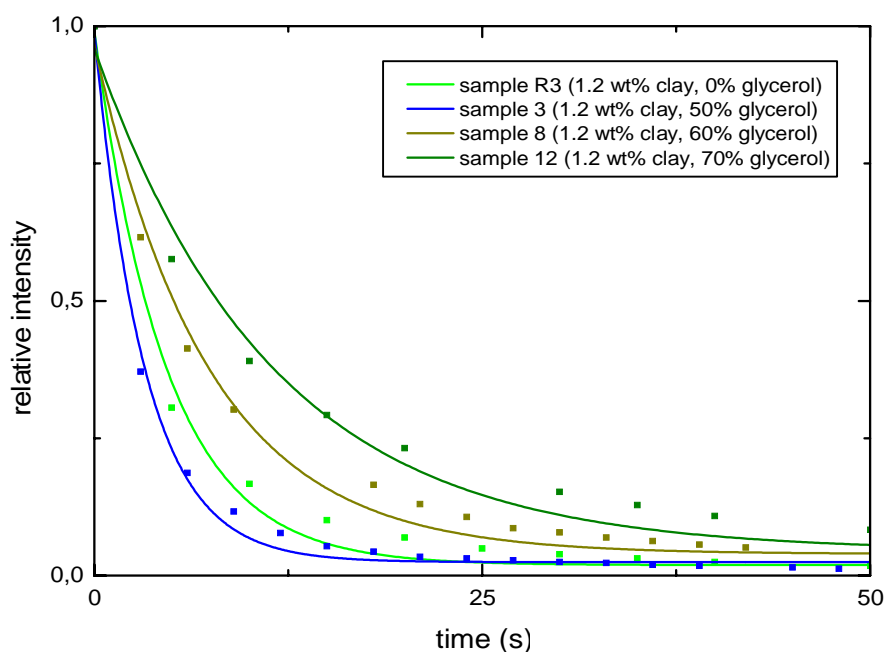


Figure 21 Relaxation of birefringence intensity as a function of time for samples with 1.2 wt% of clay and different glycerol concentration between 0 wt% to 70 wt%

The birefringence intensity relaxation was measured in the samples presented in Table 4. Figure 21 and 22 illustrate the fitting of the relaxation curves to the experimental data for different samples. The relative intensities of all tested samples decreased dramatically in the first few seconds after shaking followed by a more slow exponential decay.

The fitted relaxation exponential times are plotted in Figure 23 and 24. Figure 23 shows that at a constant clay concentration of 1.2 wt% an increase in glycerol concentration from 0 to 50 wt% resulted in a shorter relaxation time. When the glycerol concentration was increased from 50 to 70 wt% the relaxation time increased sharply. Furthermore, Figure 24 shows that samples with 1.6 wt% clay have longer relaxation time than those only have 1.2 wt% clay. Similarly, samples with 60 wt% glycerol need longer time to relax than samples with 50 wt% glycerol. All quantitative results obtained from the relaxation measurements are consistent with the qualitative results observed the phase diagrams in Figure 7 and 8.

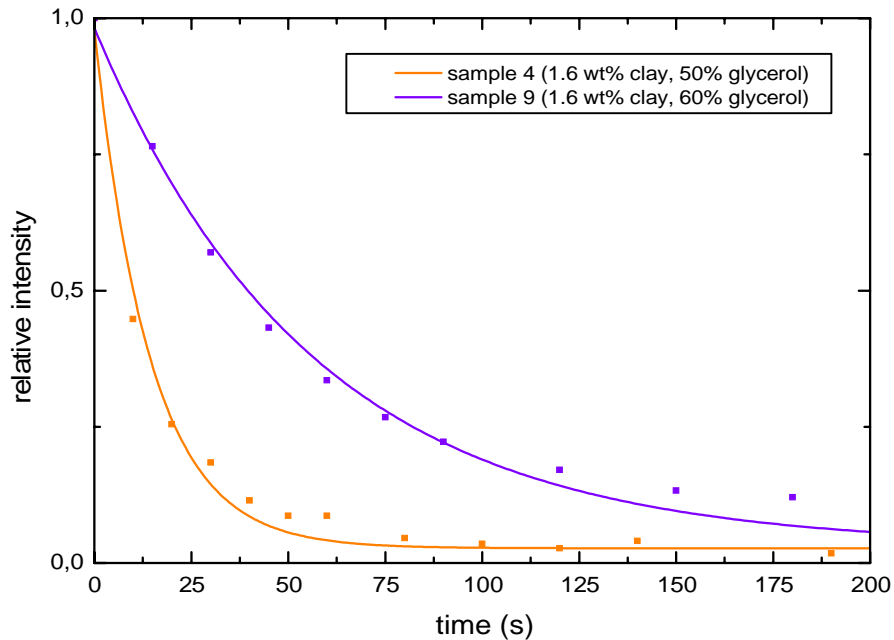


Figure 22 Relative birefringence intensity versus time for samples with a clay concentration of 1.6 wt% and 50 and 60 wt% of glycerol.

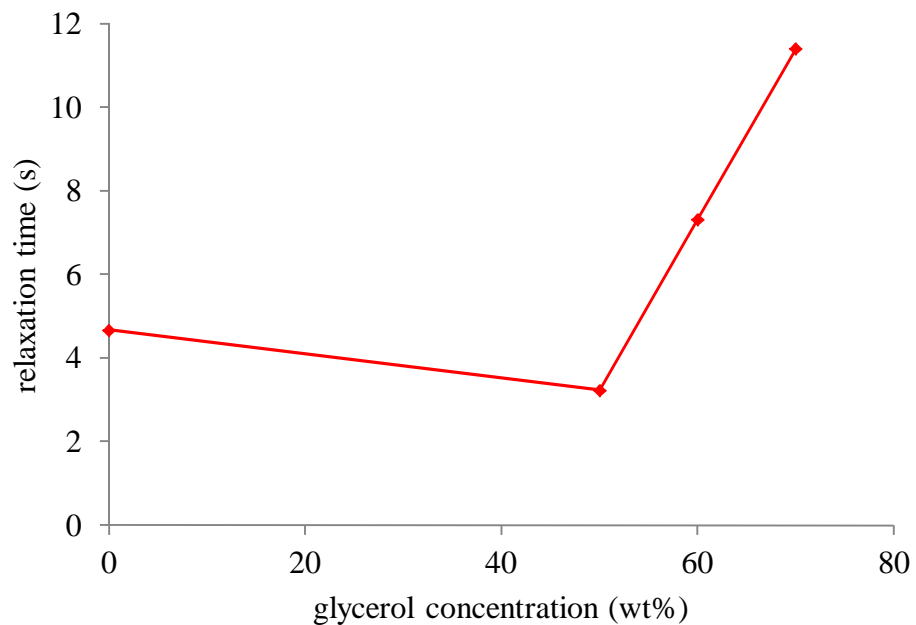


Figure 23 Relaxation time as a function of glycerol concentration for samples with 1.2 wt% clay.

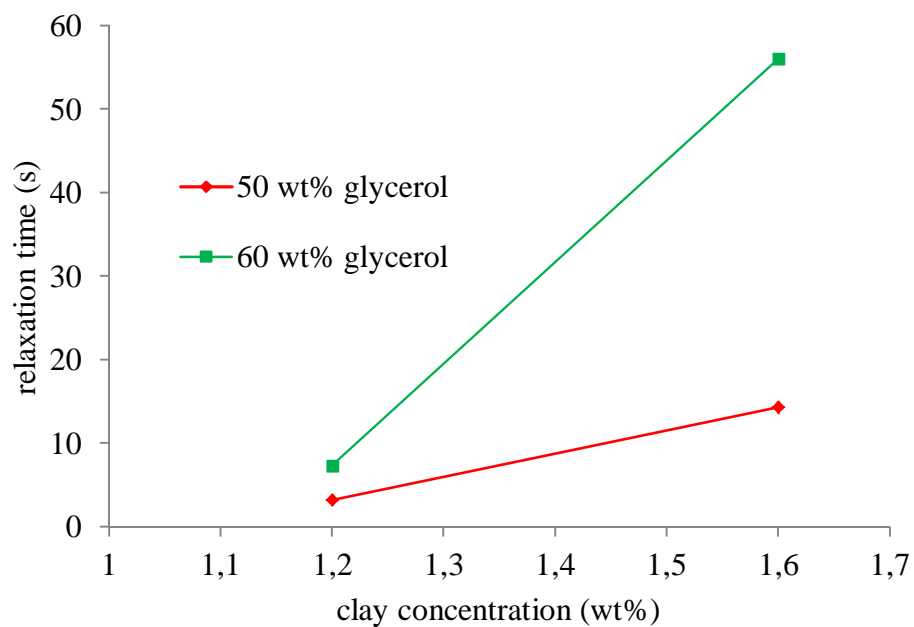


Figure 24 Relaxation times as a function of clay concentration for samples with different glycerol concentrations.

4.2 Colloidal system consisted of NAu s2 clay and aqueous PMAAm dispersion

In this part, pure PMAAm dispersions and magnetic alignment of clay particles in clay-PMAAm dispersions in Table 2 were investigated, the results are shown below.

4.2.1 Behaviours of PMAAm

In Figure 25 the pure polymer PMAAm solutions and the effect of temperature are shown. The images of the hot solutions were taken immediately after samples had been heated to 75°C after which the samples became transparent. When cooled the samples became opaque with a white cloudiness. It is not obvious in the images, but the sample with 3 wt% polymer was whiter than the 1 wt% sample. After 2 days the 1 wt% polymer sample was phase separated where the upper part of the sample became transparent and lower part remained white. The phase separation where even more pronounced in the 3 wt% solution as all polymers had precipitated. After 5 days the polymer in the 1 wt% sample also precipitated while the solution above the sediment was transparent. Imaging between crossed polarizers revealed no anisotropic microstructure in the samples at room temperature as the samples were of dark appearance, see Figure 25. Hence the polymer by itself does not cause any birefringence.



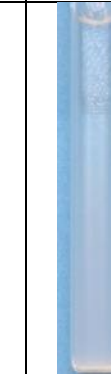




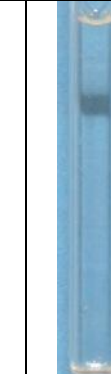












































Status Polymer content	Hot	Cooling	After 2 days	After 5 days	Between crossed- polarizers
1 wt%					
3 wt%					

Figure 25 PMAAm UCST behaviours at different temperatures and as observed between crossed polarizers. The black shadow in the square tubes is the shadow of the liquid surface.

4.2.2 *Observation of samples before and after magnetization at different temperatures*

Figure 26 shows the effect of magnetic alignment of N/Au s2 clay-PMAAm dispersions at low and high temperature. Before magnetization, the 1.5 wt% pure clay sample showed a slight birefringence after shaking. The addition of polymer meant that the birefringence disappeared in all samples with 1.5 wt% clay. After magnetization, the samples were aligned by the magnetic field and the intensity of the birefringence decreased with increasing polymer concentration. At this clay concentration there were no obvious differences in birefringence intensity at high and low temperature.

(a)		Polymer concentration (wt%)						
		0	0.5	1	1.5	2	2.5	3
1.5 wt% clay	Before magnetization							
	After magnetization at 25°C							
	After magnetization at 75°C							

(b)		Polymer concentration (wt%)						
		0	0.5	1	1.5	2	2.5	3
2.1 wt% clay	Before magnetization							
	After magnetization at 25°C							
	After magnetization at 75°C							

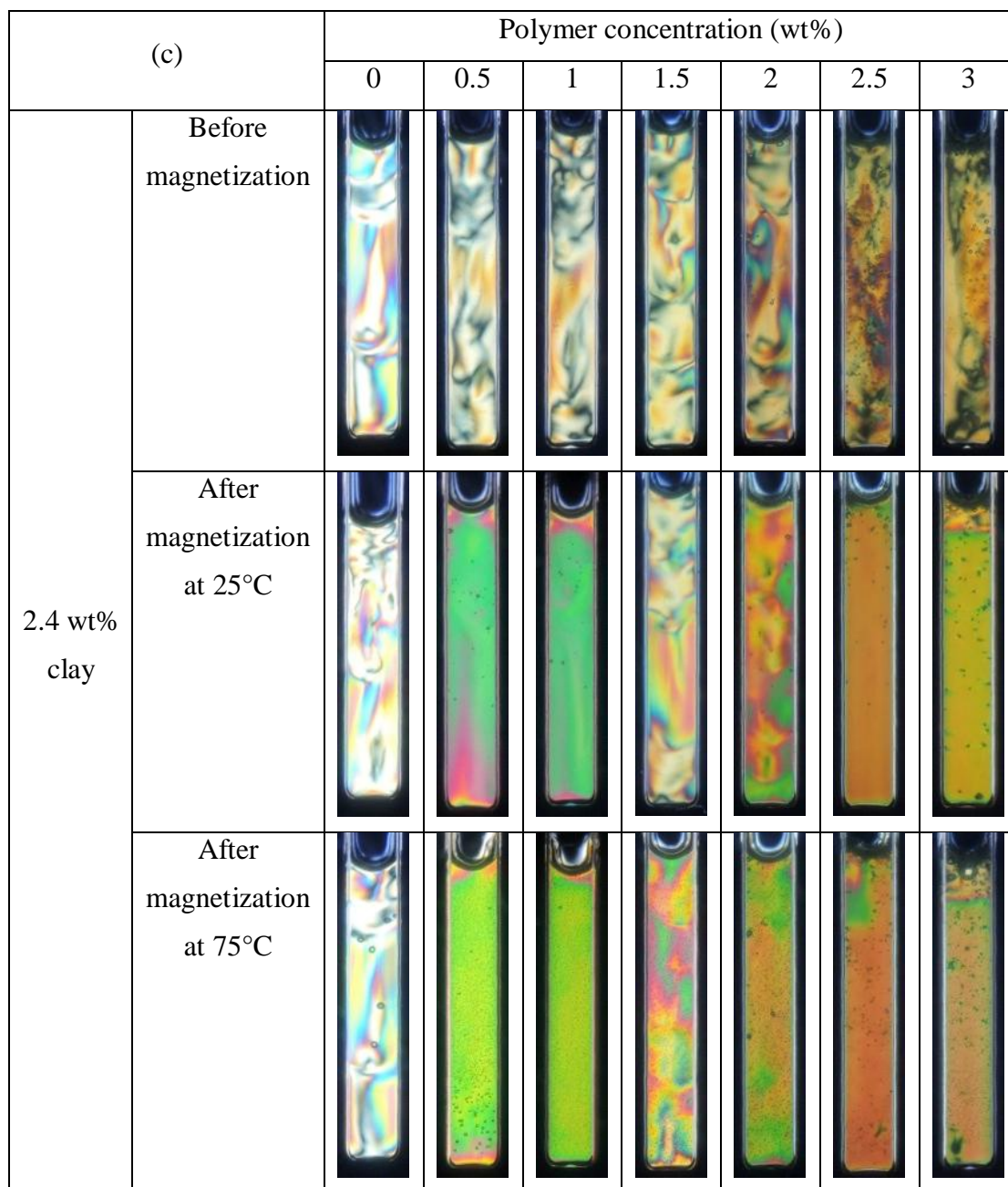


Figure 26 NAm s2 clay-PMAAm dispersions with (a) 1.5 wt% clay, (b) 2.1 wt% clay and (c) 2.4 wt% clay imaged between crossed polarizers before and after magnetization at 25 °C and 75 °C, no salt was added to the samples.

Samples with 2.1 wt% clay were also well aligned except the pure clay dispersion. The aligned samples had a homogenous birefringent appearance at both low and high temperature. There was only a small difference in birefringence intensity between 25 °C and 75 °C in the samples with 1 and 3 wt% polymer. At the other polymer concentrations the appearance was similar before and after heating.

The samples with 2.4 wt% clay and no polymer, and 1.5 and 2 wt% polymer were not aligned but the samples with 0.5, 1, 2.5 and 3 wt% polymer were. Sample with 2 wt% polymer had the

strongest birefringence difference between low and high temperature, even if it is not a large difference.

5 Discussion

Viewing Figure 4 and 5 a higher glycerol concentration in glycerol-water mixtures always produces more viscous samples. Therefore it was hypothesised that qualitatively similar correlations between the micro (birefringence relaxation time) and macro-rheological properties (rheometer measurements) would be found in systems containing glycerol, water and clay. Indeed Figure 23 shows such a correlation for increasing glycerol concentration between 50-70 wt% glycerol and Figure 24 illustrates that samples with 60 wt% glycerol experienced longer relaxation times than 50 wt%. Also, Figure 7, 8 and 24 proves that an increased clay concentration yield longer relaxation time. Interestingly, the relaxation times predicted well which samples can be aligned or not in a magnetic field. However, a comparison between relaxation times and macro-rheological properties such as viscosity at increasing clay concentration proved far from trivial as will be discussed in detail below.

5.1 Clay concentration, magnetic alignment and birefringence relaxation time

Figure 7 and 8 shows that a higher clay concentration induced higher birefringence intensity and longer relaxation time of samples after shaking. According to literature^{38, 39}, birefringence is a typical sign of nematic-like phases in clay dispersions. With increasing clay concentrations, clay dispersions show a transition from an isotropic phase to a nematic-like phase.³⁸ Figure 9 illustrates how the magnetic alignment depended on clay concentration. 0.3 and 0.8 wt% clay dispersions were dark both before and after magnetization because these samples yielded a short relaxation time due to low clay concentration as shown by Gabriel and colleagues³⁹. They found that laponite dispersion with low clay concentration had a short relaxation time. In this thesis the samples with low clay concentration relaxed immediately after they were taken out from the magnetic field and this is why these samples appeared dark between crossed polarizers. Samples with 1.2 and 1.6 wt% of clay were well aligned and birefringent, indicating that all clay particles were aligned in one direction, but these samples also had longer relaxation time according to Figure 24. Clay particles in samples with highest clay concentration (2.1 wt%) were not uniformly aligned after magnetization as the sample did not show a homogenous birefringence. This is probably because of stronger interactions between clay particles in high concentrated dispersions as it is more crowded, resulting in longer relaxation times.⁴⁰

5.2 Clay concentration, macro-rheology and its correlation to relaxation time

Figure 14 shows that the curves for G' , G'' and the relative viscosity reached a minimum at a clay concentration of 1.6 wt% when the clay concentration was varied. There are at least two possible explanations for this behaviour. The first explanation involves the appearance of nematic-like phases as the clay concentration was increased. As shown in Figure 7, the clay dispersions were nematic-like at a clay concentration of 1.2 wt% and 1.6 wt%. The formation of a nematic-like clay phase allowed for decreases of G' , G'' and relative viscosity at 1.2 and 1.6 wt%.

Similarly, Wissbrun and co-workers⁴¹ found that the G' of a thermotropic polyester is significantly higher in the isotropic phase compared to the nematic phase. This can be explained by the liquid-like behaviour of liquid crystalline phases, making it possible for these phases to move with less hindrance than an isotropic state at lower clay concentration.^{41, 42} Another explanation could be that the counter ions of the clay plates screen the clay surface charge of other clay particles at higher clay concentration. Effectively the concentration of counter ions in a volume increases with increasing clay concentration. The electrical double layer of a clay particle may be screened by these counter ions that reduces the electrostatic interaction between clay particles and further reduces rheological properties of clay dispersions. According to Abend et al.²⁰ the storage modulus (G') of Wyoming montmorillonite declined sharply as the NaCl concentration increased from 0 to 10 mM. Also, Kelessidis et al.³² reported that yield stress of bentonite dispersions decreased with increasing NaCl concentration.

Increasing the clay concentration from 1.6 wt% to 2.1 wt%, the storage and loss modulus and relative viscosity increased sharply and this is attributed to clay interparticle collisions and possible dispersion gelation. Abend and co-workers²⁰ observed similar effects when increasing the montmorillonite concentration from 2 to 4 wt%, which increased both the storage modulus and the viscosity.

As mentioned before, the relaxation time represents the micro-rheological properties of clay dispersions and the properties always increased with increasing clay concentration. However, as just discussed the macro-rheological properties measured by the rheometer did not show a simple increase with clay concentration.

5.3 Glycerol concentration, magnetic alignment and birefringence relaxation time

The birefringence observations of the phase diagrams in Figure 7 and 8 show that the addition of 50 wt% glycerol resulted in less birefringence than in the pure clay samples. Similar observations were made in samples in Figure 9 after magnetization. This is attributed to the addition of 50 wt% glycerol, which made it easier for the clay to relax from an aligned to an isotropic state as the glycerol reduced the clay-clay interaction. This was confirmed by the relaxation time measurements in Figure 23 as well. The clay-clay interaction might be reduced in any of the following ways: Firstly, the presence of glycerol can increase the interlayer spacing of clay and make clay disperse more homogeneously, partly because the glycerol is larger than the water molecule.⁴³ Secondly, glycerol decreases the dielectric constant of the solution, which is favoured for the mutual repulsion of the ionic groups.²⁹ Thirdly, the addition of glycerol may also affect the degree of association between cations and clay surfaces as glycerol is less polar than water.⁴⁴

From Figure 7 and 9, it can be seen that samples with 1.2 wt% clay and higher glycerol concentration (>50 wt%) appeared to have an increased birefringence caused by increasing solvent viscosity and slower relaxation according to Figure 4. Champion and colleagues⁴⁵ investigated the relaxation time of a single kaolinite particle in water-glycerol mixtures which

was proportional to the viscosity of the continuous phase. While planning the experiments it was hypothesised that increased viscosity of the water-glycerol mixture surrounding the clay particles would both slow down alignment and the relaxation of the clay particles. The relaxation time measurements in Figure 23 and 24 indeed prove that increasing glycerol concentration slows down the relaxation. It then follows that the alignment should be slower if the glycerol concentrations are increased. However, it is not possible to conclusively say that the alignment becomes slower as we do not observe the alignment *in situ* and in Figure 9 all samples with the same clay have similar birefringence intensity.

5.4 Glycerol concentration, macro-rheology and its correlation to relaxation time

It was hypothesised that the rheological properties of clay-glycerol dispersions would correlate well with the increase in glycerol concentration (according to Figure 4). However, the rheology results told a different story. With increasing glycerol concentration, the rheological properties of the samples with low clay concentration (0.3 wt%) in Figure 17 behaved differently compared to samples with high clay content (1.6 wt%) in Figure 20.

From Figure 17 it can be seen that the storage and loss modulus were reduced as the glycerol concentration increased from 50 wt% to 70 wt%. This could be explained by the formation of aggregates at high glycerol concentration. Although samples with 60 wt% and 70 wt% glycerol did not display aggregates visible by eye after preparation. Still, shear stress during the rheology measurements could some time induce aggregates formation which could decrease the storage and loss modulus.⁴⁶ The relative viscosity of samples did not change a lot as glycerol concentration was increased. Relative viscosity (calculated by Equation 2) was used to normalize for the viscosity caused by glycerol in itself. No change in relative viscosity with increasing glycerol concentration means that the increase in viscosity could only be attributed to the viscosity of the glycerol solution by itself. In dilute dispersions the clay particles were relative far away and they were isotropically-oriented. It could be that the glycerol affected the rheological properties of clay dispersions less in dilute clay dispersions as the clay-clay interactions did not get as pronounced under those conditions.^{41, 47}

Figure 20 shows that G' and G'' increased with increasing glycerol concentration. The cause of this could be stronger inter-particle electrostatic repulsion caused by high clay concentration.⁴⁰ In case of relative viscosity, we can see that it dropped slightly as glycerol content increases from 0 wt% to 50 wt%, then it jumped up sharply. This observation correlates well with the birefringence observations in Figure 7 and 8.

Moreover, the relative viscosity curve in Figure 20 is congruent with the relaxation time results in Figure 23. This is possible for the reasons already discussed in section 5.3. However, as mentioned in section 5.1 the relaxation time of dispersions with low clay concentration was very short,¹⁶ it was not possible to record their relaxation time to compare with their macro-rheological properties shown in Figure 17.

5.5 Sedimentation and phase separation

Figure 7, 8 and 9 illustrate that higher glycerol concentration (>70%) results in sedimentation. As apparent in Figure 8 sedimentation takes longer time when the clay concentration is increased and therefore the sediment in the sample with 0.8 wt% clay did not settle even 5 days after shaking. The upper phase is not without clay as it has a slight green colour, indicating that a fractions of the clay sediments while some stay in dispersion.

Firstly, the interaction between salt and negative charged clay surface is stronger than the hydrogen bonding between hydroxyl group and oxygen on the clay surface.^{1, 48} Moreover, the dielectric constant of glycerol is smaller than water.^{29, 49} It is possible that in clay dispersions with high glycerol concentration (>70%) the lack of water forces the clay plates to aggregate as the clay to water ratio is so high. This is similar to the scenario where clay particles start to aggregate in aqueous dispersions because the clay concentration is really high.⁵⁰

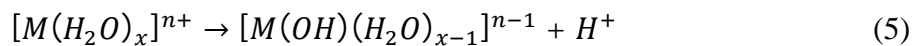
5.6 Influence of salt for magnetic alignment and relaxation time

At high salt concentration (> 0.01 M NaCl) clay dispersions usually flocculate or gel.² Figure 9 and 10 shows that a small amount of salt (10^{-4} M NaCl) can induce large changes in phase behaviour. Yet in that case it appears as if the samples gel at a lower clay concentration in the absence of salt. The increased relaxation time (not measured for the samples in Figure 10) preserves the clay alignment after magnetic exposure for a longer time compared to the samples with salt in Figure 9. DLVO theory can explain such behaviour. In dispersions with high clay concentration the clay plates that were surrounded by an electric double layer are close to close-packing. According to Abend et al.²⁰ the addition of salt can reduce the extension of the electric double layer and as a result the clay plates are not as closely packed any more, which reduced the repulse interactions, making magnetic alignment easier in the presence of a small salt concentration. As expected the macro-rheological properties indicated a more fluid sample when a small amount of salt was added.³²

5.7 Variation of pH in clay-glycerol dispersions

The pH of samples is decreasing with higher clay concentration and had a significant drop caused by adding glycerol.

Marshall and colleagues⁵¹ found that the titration curves of electro-dialysed montmorillonite were similar to those of ordinary weak acids. The reason could be that OH groups on the outer surfaces are weakly ionized. The acidity of clays is generated from H^+ ions which occupy exchange sites on the surface or by dissociation of the water hydrating the exchangeable metal cations as⁵²



After adding glycerol, the pH value of clay dispersions dropped significantly. Here it might be assumed that the presence of glycerol promotes the ionization of OH groups on the clay surface.

5.8 PMAAm concentration, magnetic alignment and birefringence relaxation time

The aim of these experiments was to formulate a system in which the clay orientation could be changed after heating the samples and then the clay orientation was supposed to be fixed by cooling the sample to room temperature. In Figure 26 dilute clay samples with 1.5 wt% clay and different polymer concentration could all be aligned by a magnetic field at both high and low temperature. However the relaxation time of the samples decreased with increasing polymer concentration. The polymer molecules seems to disturb the interaction between clay particles, which is similar to what was observed with glycerol.^{29, 43, 45}

The dispersion with 2.1 wt% pure clay could not be aligned at low or high temperature but samples with PMAAm showed homogenous birefringence appearance. This could also be explained by the disturbance of polymer molecules as mentioned above. The different colours of birefringence observed in the 2.1 wt% clay samples with various PMAAm concentrations could be due to different degree of alignment of the clay particles which changes the sample birefringence. The colours and birefringence could possibly be interpreted with a Michael-Levy birefringence chart⁵³ however complementing experiments would be needed.

In samples with a clay concentration of 2.4 wt%, samples with 1.5 and 2 wt% PMAAm could not be aligned homogenously. This complex clay alignment - polymer concentration behaviour needs further investigation before any conclusions can be drawn.

6 Conclusion

In this project, the magnetic alignment and relaxation of nontronite particles were investigated in both aqueous glycerol and PMAAm solutions. Two factors, clay concentration and glycerol/PMAAm concentration were varied in the experiments. Increasing clay concentration caused stronger birefringence, more difficult magnetic alignment and longer relaxation time. Interestingly, adding glycerol or increasing PMAAm concentration reduced relaxation time and made alignment easier. However, if the glycerol concentration was increased further (>50 wt%), the birefringence intensity and relaxation time increased because of higher solvent viscosity. Furthermore, the rheological properties of clay-glycerol dispersions were measured to study the relationship between the micro- and macro-rheological behaviours of this anisotropic material. It has been found that there was a sharp drop of G' , G'' and relative viscosity when NAm s2 clay concentration increased to 1.6 wt%, probably due to the nematic-like phase formed in high concentrated clay dispersions. The relative viscosity of samples with high clay content showed good correlation with the relaxation time measurements, which also proved the disturbance or reduction effect caused by glycerol.

The UCST polymer PMAAm did not lock the clay particles into position when exposed to a magnetic field, instead it was possible to align the clays at all temperatures, even if there were indications of easier alignment at high temperature. It might be that higher polymer concentration is needed to archive the desired effect. However, limitations in water solubility of the UCST-polymer used in this study make it hard to reach a higher polymer concentration. To achieve a higher polymer concentration it is likely that another type of UCST-polymer is needed. More studies of the thermoresponsive polymer combined with clay in this anisotropic material are required to reach the final purpose which is changing the permeability by magnetic field and temperature.

Acknowledgements

I would like to express my deepest appreciation to my supervisor, Christoffer Abrahamsson, who has the substance and the attitude of a genius. Without his guidance and persistent help this dissertation would not have been possible.

I would like to thank my examiner, Professor Michael Persson, who has given his valuable time, advice, criticism and made corrections to this thesis.

I would like to thank Professor Magnus Nydén, who gave me the opportunity to do research in his lab at the University of South Australia, and also his useful feedback and guidance regarding this thesis.

Great thanks to Professor Johan Bergenholtz for his help with the rheometer experiments and data analysis.

Many thanks to Dr. Mikael Larsson and Dr. Melanie Ramiasa for their aid and direction during my time in Australia, and PhD student Alexander Idström for allowing us to use his nice Nikon camera. A special thanks to Hanzhu, who has provided spirit and cooking support in during the past year.

To all relatives, friends and others who in one way or another gave their support, thank you.

References

1. O. Sobolev, F. Favre Buivin, E. Kemner, M. Russina, B. Beuneu, G. Cuello and L. Charlet, *Chemical Physics*, 2010, **374**, 55-61.
2. C. Abrahamsson, L. Nordstierna, J. Bergenholtz, A. Altskär and M. Nydén, *Soft matter*, 2014, **10**, 4403-4412.
3. Y. Kojima, A. Usuki, M. Kawasumi, A. Okada, T. Kurauchi, O. Kamigaito and K. Kaji, *Journal of Polymer Science Part B: Polymer Physics*, 1995, **33**, 1039-1045.
4. G. Maitland, *Current opinion in colloid & interface science*, 2000, **5**, 301-311.
5. C. Aguzzi, P. Cerezo, C. Viseras and C. Caramella, *Applied Clay Science*, 2007, **36**, 22-36.
6. Z. Gerstl, A. Nasser and U. Mingelgrin, *Journal of Agricultural and Food Chemistry*, 1998, **46**, 3803-3809.
7. Z. Gerstl, A. Nasser and U. Mingelgrin, *Journal of Agricultural and Food Chemistry*, 1998, **46**, 3797-3802.
8. R. Pashley and M. Karaman, *Applied colloid and surface chemistry*, John Wiley & Sons, 2005.
9. J. Duncan, Butterworth, Heinemann, 1992.
10. S. Lin and M. R. Wiesner, *Langmuir*, 2012, **28**, 15233-15245.
11. M. Romero-Cano, A. Puertas and F. De las Nieves, *The Journal of Chemical Physics*, 2000, **112**, 8654-8659.
12. L. J. Michot, I. Bihannic, S. Maddi, S. S. Funari, C. Baravian, P. Levitz and P. Davidson, *Proceedings of the National Academy of Sciences*, 2006, **103**, 16101-16104.
13. E. Tombacz and M. Szekeres, *Applied Clay Science*, 2004, **27**, 75-94.
14. L. J. Michot, I. Bihannic, S. Maddi, C. Baravian, P. Levitz and P. Davidson, *Langmuir*, 2008, **24**, 3127-3139.
15. L. J. Michot, C. Baravian, I. Bihannic, S. Maddi, C. Moyne, J. F. Duval, P. Levitz and P. Davidson, *Langmuir*, 2008, **25**, 127-139.
16. J. C. Gabriel and P. Davidson, *Advanced Materials*, 2000, **12**, 9-20.
17. A. Shahin, Y. M. Joshi and S. A. Ramakrishna, *Langmuir*, 2011, **27**, 14045-14052.
18. S. Sinha Ray and M. Okamoto, *Progress in polymer science*, 2003, **28**, 1539-1641.
19. J. Mewis and N. J. Wagner, *Advances in Colloid and Interface Science*, 2009, **147**, 214-227.
20. S. Abend and G. Lagaly, *Applied Clay Science*, 2000, **16**, 201-227.
21. R. Schofield and H. Samson, *Discussions of the Faraday Society*, 1954, **18**, 135-145.
22. J. Gooch, *Atlanta, USA: Springer Science+ Business Media*, **200**, 772.
23. J. B. Segur and H. E. Oberstar, *Industrial & Engineering Chemistry*, 1951, **43**, 2117-2120.
24. N.-S. Cheng, *Industrial & engineering chemistry research*, 2008, **47**, 3285-3288.
25. A. Silberberg, J. Eliassaf and A. Katchalsky, *Journal of Polymer Science*, 1957, **23**, 259-284.
26. J. Seuring and S. Agarwal, *Macromolecular rapid communications*, 2012, **33**, 1898-1920.
27. P. F. Luckham and S. Rossi, *Advances in Colloid and Interface Science*, 1999, **82**, 43-92.
28. J. Israelachvili and R. Pashley, 1982.
29. C. Carnero Ruiz, L. Diaz-Lopez and J. Aguiar, *Journal of colloid and interface science*, 2007, **305**, 293-300.

30. M. Butterworth, L. Illum and S. Davis, *Colloids and Surfaces A: Physicochemical and Engineering Aspects*, 2001, **179**, 93-102.
31. L. Onsager, *Annals of the New York Academy of Sciences*, 1949, **51**, 627-659.
32. V. C. Kelessidis, C. Tsamantaki and P. Dalamarinis, *Applied Clay Science*, 2007, **38**, 86-96.
33. H. Ohshima, *Biophysical chemistry of biointerfaces*, John Wiley & Sons, 2011.
34. M. Dijkstra, J. Hansen and P. Madden, *Physical review letters*, 1995, **75**, 2236.
35. E. Paineau, L. J. Michot, I. Bihannic and C. Baravian, *Langmuir*, 2011, **27**, 7806-7819.
36. J. Daintith, New York: Oxford University Press, 2008.
37. M. Abramowitz, W. Fester, T. Fellers, K. Spring, M. Parry-Hill, D. Murphy and M. Davidson, *Polarization of light*, 2005.
38. P. Forsyth Jr, S. Marçelia, D. Mitchell and B. Ninham, *Advances in Colloid and Interface Science*, 1978, **9**, 37-60.
39. J.-C. P. Gabriel, C. Sanchez and P. Davidson, *The Journal of Physical Chemistry*, 1996, **100**, 11139-11143.
40. L. Barclay and R. Ottewill, *Special Discussions of the Faraday Society*, 1970, **1**, 138-147.
41. K. Wissbrun and A. Griffin, *Journal of Polymer Science: Polymer Physics Edition*, 1982, **20**, 1835-1845.
42. D. MASAO, *Journal of Polymer Science: Polymer Physics Edition*, 1981, **19**, 243.
43. M. S. Beauvalet, F. F. Mota, R. M. Soares and R. V. Oliveira, *Polymer Bulletin*, 2013, 1-11.
44. S. Yariv, D. K. Ghosh and L. G. Hepler, *J. Chem. Soc., Faraday Trans.*, 1991, **87**, 1201-1207.
45. J. V. Champion, G. H. Meeten and B. R. Moon, *Journal of the Chemical Society, Faraday Transactions 2: Molecular and Chemical Physics*, 1979, **75**, 767-779.
46. J. Vermant and M. Solomon, *Journal of Physics: Condensed Matter*, 2005, **17**, R187.
47. S. W. Sofie and F. Dogan, *Journal of the American Ceramic Society*, 2001, **84**, 1459-1464.
48. W. Friedrichs, S. Köppen and W. Langel, *Surface Science*, 2013, **617**, 42-52.
49. M. Haidekker, T. Brady, D. Lichlyter and E. Theodorakis, *Bioorganic chemistry*, 2005, **33**, 415-425.
50. G. Nagelschmidt, *Journal of Scientific Instruments*, 1941, **18**, 100.
51. C. Marshall and C. Krinbill, *The Journal of Physical Chemistry*, 1942, **46**, 1077-1090.
52. P. Kumar, R. V. Jasra and T. S. Bhat, *Industrial & engineering chemistry research*, 1995, **34**, 1440-1448.
53. K. Spring, M. Parry-Hill and M. Davidson, *Olympus Microscopy Resource Center*, 2010.